# Copyright Warning & Restrictions

The copyright law of the United States (Title 17, United States Code) governs the making of photocopies or other reproductions of copyrighted material.

Under certain conditions specified in the law, libraries and archives are authorized to furnish a photocopy or other reproduction. One of these specified conditions is that the photocopy or reproduction is not to be "used for any purpose other than private study, scholarship, or research." If a, user makes a request for, or later uses, a photocopy or reproduction for purposes in excess of "fair use" that user may be liable for copyright infringement,

This institution reserves the right to refuse to accept a copying order if, in its judgment, fulfillment of the order would involve violation of copyright law.

Please Note: The author retains the copyright while the New Jersey Institute of Technology reserves the right to distribute this thesis or dissertation

Printing note: If you do not wish to print this page, then select "Pages from: first page # to: last page #" on the print dialog screen

## ABSTRACT

**QUANTIFYING PREHENSION IN PERSONS WITH STROKE POST REHABILITATION**
**by**
**Saumya Sara Puthenveettil**

This study describes the analysis of reaching and grasping abilities of the hemiparetic arm and hand of patients post stroke after a series of interactive virtual reality (VR) simulated training sessions and conventional physical therapy of similar intensity. Six subjects participated in VR training and five subjects in clinical rehabilitation for two weeks. Subjects' finger joint angles were measured during a kinematic reach to grasp test using CyberGlove® and arm joint angles were measured using the trackSTAR™ system prior to training and after training. Downward force applied to the object during grasping was assessed using Nano17™, a force/torque sensor system that is added to the reach to grasp test paradigm for the VR trained subjects. Results from total movement time, grasping time, and average applied force show that subjects significantly decreased their average kinematic times and force applied to object during reaching and grasping tasks. Classification of hand postures using Linear Discriminant Analysis (LDA) during the reaching phase of movement shows an improvement in subjects' accuracies and abilities to preshape their fingers post training in both groups. A system utilizing magnetic trackers, a data glove, and a force sensor is sensitive to changes in motor performance elicited by a robotically facilitated, virtually simulated motor intervention and physical therapy of similar intensity.

# QUANTIFYING PREHENSION IN PERSONS WITH STROKE POST REHABILITATION

**by**
**Saumya Sara Puthenveettil**

**A Thesis**
**Submitted to the Faculty of**
**New Jersey Institute of Technology**
**in Partial Fulfillment of the Requirements for the Degree of**
**Master of Science in Biomedical Engineering**

**Department of Biomedical Engineering**

**May 2012**

**APPROVAL PAGE**

**QUANTIFYING PREHENSION IN PERSONS WITH STROKE POST REHABILITATION**

**Saumya Sara Puthenveettil**

---

Dr. Sergei V. Adamovich, Thesis Advisor — Date
Associate Professor of Biomedical Engineering, NJIT

---

Dr. Richard A. Foulds, Committee Member — Date
Associate Professor of Biomedical Engineering, NJIT

---

Dr. Max Roman, Committee Member — Date
Assistant Research Professor of Biomedical Engineering, NJIT
Director, MS Program

## BIOGRAPHICAL SKETCH

**Author:** Saumya Sara Puthenveettil

**Degree:** Master of Science

**Date:** May 2012

**Undergraduate and Graduate Education:**

- Master of Science in Biomedical Engineering,
  New Jersey Institute of Technology, Newark, NJ, 07102, 2012

- Bachelor of Science in Mechanical Engineering,
  Rensselaer Polytechnic Institute, Troy, New York, 12180, 2007

**Major:** Biomedical Engineering

## ACKNOWLEDGMENT

The author would like to thank her thesis advisor Dr. Sergei Adamovich for his support in the completion of this study. She is also thankful to be involved in research with the NeuroRehabilitation laboratory as the topic of her thesis.

Special thanks to Dr. Max Roman and Dr. Richard Foulds for serving as committee members for this thesis.

The author is also grateful to the University of Medicine and Dentistry of New Jersey and JFK Johnson Rehabilitation Institute for their support during data collection.

Finally, the author offers her gratitude to Gerard Fluet and Qinyin Qiu from the NeuroRehabilitation laboratory at NJIT for their support and friendship.

## TABLE OF CONTENTS

**TABLE OF CONTENTS**
**(Continued)**

## LIST OF TABLES

## LIST OF FIGURES

## LIST OF DEFINITIONS

| | |
|---|---|
| Kinematic | The analysis of angles and motion of bodies |
| DIP | Distal Interphalangeal |
| PIP | Proximal Interphalangeal |
| MCP | Metacarpophalangeal |
| TMJ | Trapeziometacarpal Joint |
| Ataxia | Lack of coordination of movement |
| Hemiparesis | Neurological condition affecting stroke subjects causing weakness on one side of the body |

# CHAPTER 1

# INTRODUCTION

## 1.1 Objective

The objective of this thesis is to quantify and compare hand preshaping and grasping abilities in stroke subjects who participated in two types of interventions for the hemiparetic arm and hand: interactive virtual reality (VR) simulated training and clinical rehabilitation training of similar intensity. This study describes the design and testing of a system aimed at quantifying improvement in reaching and grasping abilities of the hemiparetic arm and hand of post stroke patients after a series of training sessions. Six subjects participated in VR training and five subjects in clinical rehabilitation consisting of repetitive task practice (RTP) for two weeks. Kinematic finger joint angle measurements and wrist positions were obtained using CyberGlove® and trackSTAR™ systems pre and post training. Force measurements were obtained using Nano17™, a force/torque sensor system pre and post training for subjects in the VR training group. This study analyzes total movement times, grasping times, maximum vertical force applied to the object during grasping, classification of finger joint angles during hand preshaping, and correlations between finger joint angles. Preshaping of finger joint angles into object shape is analyzed by classifying hand postures using Linear Discriminant Analysis (LDA) in order to determine improvement in preshaping of the hand pre and post rehabilitative training. Total movement times, grasping times, maximum force, and hand preshaping accuracy are analyzed from data obtained from electromagnetic sensors, a data glove, and a force sensor system.

## 1.2 Background Information

### 1.2.1 Prehension and Previous Research

The evolution of the human hand during transport (reaching) and prehension (grasping) has been studied extensively in order to determine the underlying neural mechanisms of motor planning. Prehensile motion refers to when the hand seizes an object and holds it. Prehension requires that the object be securely held, and thus stability is essential. In order to achieve this stability, Napier classifies all human prehensile hand movements into two categories: power grip and precision grip [1]. In a power grip, the hand forms into a clamp with the palm and flexed fingers and opposing pressure by the thumb. In the precision grip, the object is pinched between the fingers and thumb.

Hand formation varies anatomically as the functional purpose of formation varies. During a power grip, the thumb is adducted at the metacarpophalangeal (MCP) and carpometacarpal joints and during the precision grip, the thumb is abducted at these joints. The degree of finger flexion and the manipulation of the palm area varies depending on the dimensions of the object. With small sized objects, the need for precision in grip becomes greater, and thus relies more heavily on the thumb and index finger digits which are well suited for fine control.

Each finger of the human hand (Figure 1.1) consists of three joints, the distal interphalangeal (DIP), proximal interphalangeal (PIP), and metacarpophalangeal (MCP). The DIP and PIP joints have one degree of freedom each and the MCP joint has two degrees of freedom. The thumb has three joints which are the interphalangeal joint with

one degree of freedom, and an MCP joint and trapeziometacarpal joint (TMJ) each with two degrees of freedom, for a total of 21 degrees of freedom [2].

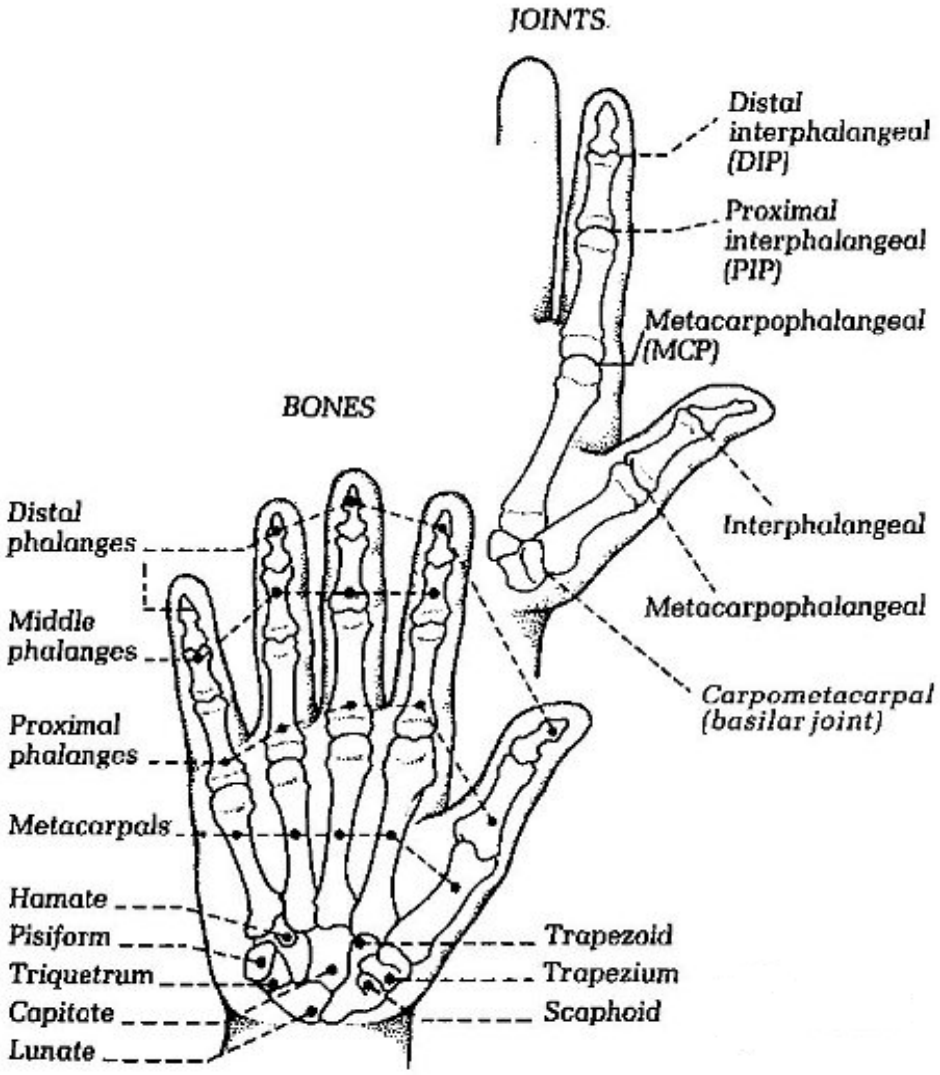


**Figure 1.1** Hand anatomy.

Source: American Society for Surgery of the Hand
http://www.assh.org/Public/HandAnatomy/Pages/default.aspx [2]

Reach to grasp tests are utilized by researchers to study human movement. Although the set up of a reach to grasp test varies from one study to another, it generally consists of a subject seated with arm and hand in a preset position. When cued, the subject is directed to reach for an object, and place it at a new position and then return to the initial position. A typical reach to grasp test consists of multiple trials with different target objects or grasp criteria. Experimentally, the transport component of movement can be measured from wrist movement, and the grasp or prehension component can be measuring from grip aperture, that is, the distance between thumb and index finger.

During a reaching and grasping task, the fingers initially straighten and the grip increases, and as the hand approaches the object, grip closes in order to match the size of the object [3]. The "maximum grip aperture" is the time in which the opening distance between the thumb and index finger is the largest. This occurs between 60-70% of the reach duration and is correlated with object size. Factors that affect grasp kinematics include size of the object, weight, texture, and fragility.

Theories on transport and prehension propose the existence of sub movements such as hand transport to object, wrist direction in space, and finger preshaping to a desired grip [4]. The hypothesis of Visuomotor Channels derived from research on monkeys describes the transport phase as possessing spatial information such as distance and direction while the grasping phase possesses information such as size and shape of object. This hypothesis states that reaching and grasping possess neural pathways which trigger specific neurons during reaching and grasping tasks.

For reaching, the primary visual cortex (V1) is connected to the primary motor cortex (M1) via the parietal occipital (PO) area and dorsal premotor cortex (Figure 1.2).

Area PO is where the location of objects is processed whereas the premotor cortex is where output or action is generated. The neural pathway for grasping in monkeys connects V1 to M1 by connecting the dorsal extrastriate (ES) cortex to the anterior intraparietal area (AIP) to reach the ventral premotor cortex. Neurons activated by hand movement were found to be concentrated in the AIP area. Area AIP is connected to area F5 in the ventral premotor cortex which has been found to be related to grasping. Interestingly, neurons in F5 show selectivity in firing depending on the hand prehension, such as precision grip versus power grip [5].

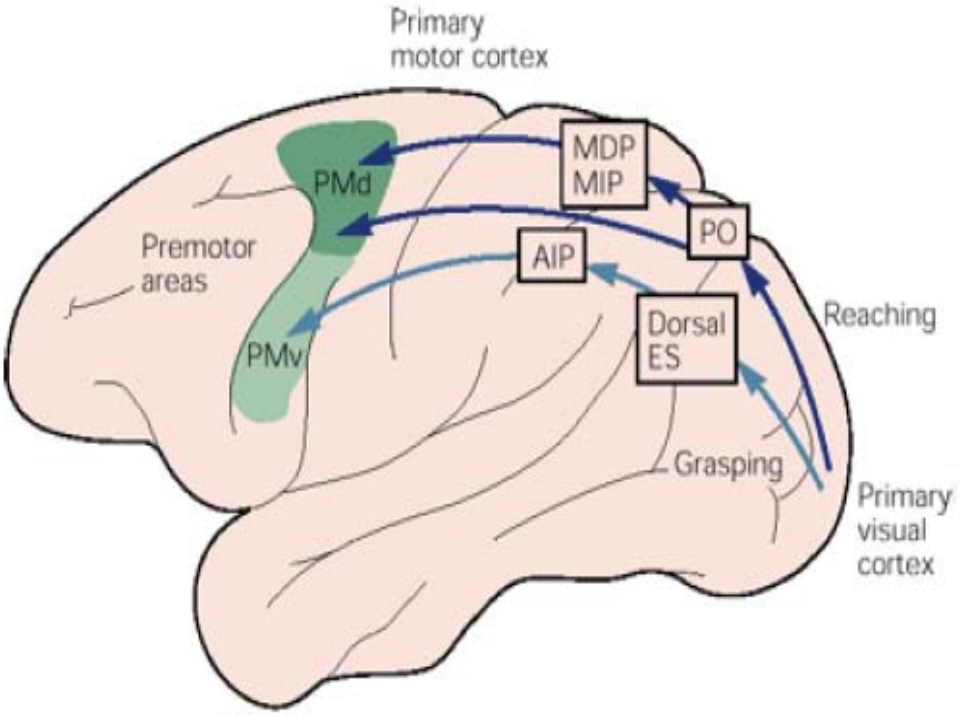


**Figure 1.2** Primary visual cortex and primary motor cortex pathways during reaching and grasping.

Source: Kandel ER, Schwartz JH, & Jessell TM (2000) *Principles of neural science* (McGraw-Hill, Health Professions Division, New York) 4th Ed, pp.1756-1779 [5]

Although there are sub movements involved in prehension, ultimately the transport and prehension phases must share a commonality in order to successfully grasp the target object. This is due to the fact that the hand must be open before the target object is reached, which elicits a temporal dependence [6]. As such, Jeannerod and other studies note that the maximum grasp size occurs during the onset of the low velocity phase preceding contact with the target object. This temporal commonality between grasp size and velocity implies that there are not only independent neural channels but also channels that work in synchrony.

Transport error refers to grasp aperture that is either the exact size of object (or exceeds the size of the object) and hand in an incorrect position. These two factors will render the hand incapable of grasping the object successfully. Wing studied expected increases in transport error because of fast transport and reaching without vision in order to relate the increase in transport error to an increase in grasp aperture. Three trials were run with subjects directed to pick up an object at normal pace, at fast pace, and with eyes closed. Results show that grasp aperture was found to be greater in fast movements and no vision movements with less accurate transport trajectories. This suggests that grasp aperture increases in order to compensate for transport errors.

According to Fitts's Law, there is a relationship between the speed and the index of difficulty of movement, in that as the movement time increases, the index of difficulty of movement increases, where the index of difficulty is the logarithm (base 2) of twice the movement amplitude divided by width of target. An increase in movement time is a function of increasing movement amplitude and decreasing tolerance, and the minimum amount of information necessary to produce movement can be calculated using these

parameters [7]. Where $I_d$ is the binary index of difficulty, $W_s$ is the tolerance, and A is the amplitude, Fitts's law is:

$$I_d = -log_2 \frac{W_S}{2A} \text{ bits/response} \quad (1.1)$$

Fitts's law can be applied to prehension in that as the object width increases, movement time increases [8]. Bootsma *et al* tested Fitts's law applied to prehension by studying the effect of amplitude, object width, and object size on movement time. Sixteen blocks of varying sizes and widths were used for this study where subjects were asked to pick up the objects at two different movement amplitudes (distance from starting to target object). Total movement time was divided into the acceleration phase from the onset of movement to the peak velocity, and the deceleration phase, from the peak velocity until the hand motion reverses (after capturing object). Results show that smaller object widths result in longer movement times caused by a longer deceleration phase and larger movement amplitude resulted in longer movement times. Object size did not have an effect on movement time as long as the size does not approach the maximum size the subject can grasp. Results from applying Fitts's law to prehensile movement show that the movement time increases as the index of difficulty increases.

Other prehension studies observe the effects of target velocity and how the velocity of a moving target affects the coupling of the transport and grasping phases. The question is whether target velocity affects only grasping, or both reaching and grasping [9]. In this study, subjects were positioned in front of a track and asked to reach for and lift a cylindrical force transducer (moving target) when it approached at various velocities from a fixed distance and from varying distances (constant viewing time). Results show

that when distance was constant and as the velocity increased, the movement time decreased. However, with constant viewing time, movement time was unaffected. Additionally, as target velocity increased, the peak aperture increased in both conditions. This study demonstrates that target motion affects both the reaching and grasping components of movement. Interestingly, when viewing time was held constant, reaching kinematics were not affected by changing target velocity. Therefore, target velocity may not affect the information offered in generating transport commands when viewing time is constrained, whereas the amount of time the subject spends viewing the target offers more information. This brings to light the significance of temporal information during a reaching action. In the preshaping mechanism, as the target's velocity increased, there is an increase in the peak aperture and peak aperture velocity.

Prehension studies have been conducted in monkeys in order to serve as a model for human prehension and motor patterns [10]. In comparing the two species, both exhibit a peak velocity during the reaching phase and a maximum grip size that decreases upon grasping. In order to study the effects of varying the size of the target object and the location, three Macaque monkeys were trained to reach for and grasp objects. In the varying size trials, two cylinders of varying diameters, one small and one large were presented, and in the varying location trials, three identical objects were presented at different locations. Reaching components were measured using wrist markers (infrared light-emitting diodes) and grasping components were measured using markers on the thumb nail and index finger. Markers were also attached to the middle finger in order to measure the distance between the thumb and middle finger. As expected, wrist velocity profiles were bell shaped and the maximum grip apertures occurred after the peak

velocity. Results show that movement times were longer for the small object than the large object and object size and location do have an effect on reaching and grasping.

In studying the preshaping component of the transport phase, a pioneering study tested the hypothesis that the hand molds to the contours of the object at the time of contact with object [11]. Subjects grasped fifteen different objects of approximately the same size but varying in shapes (convex or concave). Six subjects began each trial with their hand in an initial position for a total of ten trials. CyberGlove® (Virtual Technologies) was used to measure hand posture of the joint angles. Joint angles measured include the metacarpophalangeal (MCP) and proximal interphalangeal (PIP) of the index, middle, ring, and little fingers. The goal of this study was to distinguish between postures throughout movement. Discriminant functions computed from eigenvectors of the ratio of between groups covariance matrix to within groups covariance matrix were used to project the hand posture onto discriminant space. The minimum distance between hand postures was used to match hand posture with object shape. Results show that during reaching, between 30% to 70% of movement, fingers initially extend to maximum and then flex as the hand reaches the object. Hand postures varied according to object shape. After the peak hand aperture, hand shapes become gradually distinguishable, which takes place before the contact with the object.

Another interesting study examined the effects of visual feedback and object shape on hand preshaping [12]. The evolution of hand preshaping was studied in order to determine temporal differences of varying object shapes against full vision, vision of only the target object, and no vision conditions. The purpose of this study was to determine when distinguishable hand configurations were present and if visual feedback affected

the hand's ability to preshape or if this is only affected by object shape regardless of visual feedback. Subjects were presented three objects of varying shapes and widths. A data glove was employed and individually calibrated to obtain measurements of MCP and PIP joint angles. Subjects were asked to reach to and grasp objects when cued. In the 'object vision' condition, the room was completely darkened and only the objects were visible, which were painted light-green and fluorescent. In the 'no vision' condition, subjects performed reach to grasp trials with eyes closed. Position of wrist was measured using electromagnetic sensors. Due to the inability to accurately measure thumb position using the data glove, the maximum aperture was calculated as the distance between the tip of the index finger and perpendicular finger displacement (index finger displacement) defined as:

$$IFD = L1\cos\alpha + L2\cos\beta \quad (1.2)$$

L1 and L2 are the lengths of individual subjects' index finger phalanges, α and β are the flexion angles of the MCP and PIP joints. Canonical discriminant analysis was used to obtain classification errors of hand preshaping as the hand reached for the object. The classification error is defined as the incorrectly classified data or data that is placed into the wrong group (misclassifications). Results show that object shape affects hand posture throughout movement in all vision conditions, even the no vision condition. This indicates the use of information regarding object shape in grasping, which is referred to as the early predictive phase. Results also show that low classification errors were attained before 50% of movement time. Results suggest that hand preshaping consists of both an early phase and late phase. The early phase is a predictive phase where hand formation is selected while during the late phase, grasp on the object is optimized.

Reach to grasp experiments have also been advantageous in studying prehension of subjects with neurological disorders. In the case of Parkinson's disease (PD), subjects exhibit several motor impairments. Among these impairments are tremor and bradykinesia (slow movement) and PD patients show significant impairment in synchronizing their movement [13]. Hand preshaping impairment was studied in PD subjects using three different object shapes. For this study, ten PD patients and eight control subjects were employed with the hypothesis that PD subjects would have difficulty with preshaping during the reaching phase as compared to controls and would rely on visual feedback in order to accomplish this. Results show that PD subjects' movement time is significantly higher than normal controls. Additionally, mean peak velocity of the wrist is significantly lower for PD subjects than for normal controls. Analysis of classification error rates of hand preshaping in PD subjects versus normal controls shows that after 35% of movement, control subjects' classification error decreases with a steeper slope than PD subjects' classification error at that time. Additionally from 55% to 95% movement time, PD subjects' classification error was significantly higher than that of normal controls. Both groups however display a steadily decreasing classification error as hand reaches object, and so the higher classification error among PD subjects suggests a delay in their ability to preshape their hand to match the object shape

### 1.2.2 Stroke and Neurorehabilitation

Every year, approximately 800,000 people suffer from stroke, leading to long term disability or death [14]. Stroke is the loss of brain functioning due to a lack of blood flow in the brain resulting from a blockage or hemorrhage. Following stroke, upper extremity functioning is impaired in varying degrees from mild to severe levels of hemiparesis. Hemiparesis is characterized by weakness on one side of the body. These impairments can consist of slower reaction times, muscle weakness, lack of motion, and motor control of limbs.

One study aimed to research kinematic measurements that discriminated between normal and impaired motor functioning while drinking from a glass [15]. Normal subjects and subjects with hemiparesis as a result of stroke participated in a reaching task where they were instructed to reach for a drinking glass and take a sip. Compared with normal subjects, stroke subjects had significantly slower total movement times and velocity profiles for stroke subjects were more oscillatory than those of healthy subjects.

Other studies utilizing reach to grasp tests comparing stroke subjects with healthy subjects also found that stroke subjects had higher movement times than healthy subjects and lower peak velocities [16]. Stroke and other neurological disorders have inspired research in the field of neurorehabilitation in order to investigate plasticity of the human brain and recovery of function. This is because dramatic recovery can be seen in the nervous system following brain injury. Plasticity generally refers to modification of neural connections and organization among neurons. For example with stroke, substantial improvement in motor function has been seen to occur in the first thirty days and more impaired subjects can continue to improve up to ninety days [17] prior to

rehabilitation. Recovery of function refers to the individual's ability to reacquire movement skills following injury.

According to the theory of viscariation, in response to injury, the brain can reorganize such that one part of the brain can substitute for another in order to support lost functionality. This neural reorganization is believed to support recovery of motor functioning post injury. The phenomenon known as motor adaptation refers to the modification of one's movement as a result of repetition across multiple trials [18]. During this adaptation, the brain is believed to modify its movement in order to minimize the amount of energy, force, or inaccuracy of the movement. Motor learning studies investigate how movement is modified among normal individuals.

In the 1970's, Richard Schmidt proposed the schema theory of motor learning which states that there are generalized sets of rules for spatial and temporal planning involved in movement termed the generalized motor program. He proposed that after an individual makes a movement, there are four movement characteristics that are stored in short-term memory: (1) movement conditions such as position and weight of the object (2) generalized motor program (3) the results of the movement (4) sensory information about the movement : how it feels, looks, and sounds. After storage into short-term memory, two schemas are created: recall schema (motor) and recognition schema (sensory) [19]. A prediction from schema theory is that as a particular movement is practiced, by varying the movement practice, motor learning will improve.

Motor adaptation or motor learning can be facilitated with rehabilitative therapies. In constraint-induced movement therapy (CIMT), the less affected or unimpaired extremity is constrained and the impaired limb is practiced. In a study comparing CIMT

with a less intensive motor intervention, CIMT subjects showed decreased cerebral activation implying the subjects' abilities to more effectively recruit motoneurons to produce movement. As a result, after therapy, CIMT subjects' activation patterns more closely resembled that of normal volunteers. Patients have also reported a decreased effort in producing movement post therapy [20].

In a particular study, enhanced physical therapy was tested in stroke subjects who received more than twice the regular amount of physical therapy for the impaired arm along with behavioral therapy [21]. Results show that after six months, subjects in the enhanced physical therapy group among the mild group attained better arm function than those in the conventional physical therapy group, however the reverse was true for the severe group. Due to the complexity of sensorimotor control involved in reaching and grasping tasks, even slight impairment of this control can adversely affect daily living. In recent years, interventions for stroke rehabilitation include virtual reality training environments and robotic technology that utilize plasticity of the nervous system to promote recovery for hemiparesis.

Robot facilitated therapy has been investigated in order to determine whether exercising the subjects' impaired limb can promote motor recovery [22]. Robot assisted "video-games" were designed that promoted upper-limb motor recovery such as for shoulder or elbow motion. Results from clinical tests show that patients improved in motor functioning to a greater degree than those in the control group. The New Jersey Institute of Technology's (NJIT) NeuroRehabilitation lab has successfully developed VR training environments using the HapticMaster robotic arm and CyberGlove® in order to create realistic and interactive training environments to rehabilitate persons with stroke.

The HapticMaster robotic arm is a six degree of freedom (X, Y, Z, Pitch, Yaw, and Roll) force controlled robotic arm and CyberGlove® is a data glove that obtains finger joint angle measurements. Merians *et al* employed subjects with hemiparesis due to stroke to participate in a virtual reality simulated training program [23]. CyberGlove® and the Rutgers Master II-ND (force feedback glove) were connected to a PC that ran VR simulations providing continuous feedback about finger performance. An algorithm increased the subject's target goals for extension, flexion, and kinematic parameters when the subject's performance improved. Results show that subjects improved in their fractionation, motion, and speed. Another study employed four different virtual simulations, including a VR piano session, that trained repetitive extension/flexion of fingers and shoulder as well as required subjects to reach forward utilizing trunk motion [24].

VR training for subjects post stroke has resulted in improvement of the subjects' overall movement path as well as kinematic measurements. The advantages of the virtual reality simulation is that it is interactive and challenging, providing feedback to the subject. This approach to training has resulted in improvements in kinematic measurements along with improvements in finger fractionation (degree of finger independence), finger strength, and improvement in clinical tests of upper extremity function [25, 26].

This thesis will analyze changes in reaching and grasping abilities of persons with stroke subsequent to a program of VR training and an equivalent program of conventional physical therapy of similar intensity, using the reach to grasp paradigm. The aims of this thesis is first (i) to study the effects of VR rehabilitation training sessions on

the vertical force applied to a target object during a reach to grasp test, (ii) to study the effects of both VR rehabilitation and clinical rehabilitation on the kinematics of reaching and grasping; movement time and grasping time (iii) to determine whether rehabilitation improves the ability to distinguish between hand postures in the hand preshaping phase (iv) to compare correlations of finger joint angles of the unimpaired right hand of subjects to that of previous literature.

# CHAPTER 2

# IMPLEMENTATION

## 2.1 Subjects and Apparatus

This study is a subset of ongoing research at the NeuroRehabilitation lab at NJIT which is supported in part by NIH grant HD 58301 and by the National Institute on Disability and Rehabilitation Research RERC grant #H133E050011. Eleven subjects post stroke, average age 53, three females and eight males with mild to severe hemiparesis were recruited for this study. The subjects in this study suffered from hemiparesis; their hemiparesis occurred on the side of the body opposite to the side of the brain where the lesion occurred. Six subjects were virtual reality trained and five subjects were trained with conventional physical therapy. Six subjects trained their hemiparetic hand with interactive virtual reality (VR) computer games and five subjects trained their hemiparetic hand with a program of non-automated repetitive task practice (RTP). Force measurements for five subjects were acquired during the reach to grasp tests. These subjects are the VR group subjects since the force sensor was not available for data collection until a later date. Joint angle measurements during reach to grasp tests were acquired for ten subjects since there was an error in data collection for one subject from the VR group. For classification, four subjects from the RTP group were selected for comparison with four subjects from the VR group. Wrist kinematic data was acquired for all eleven subjects.

Subjects sat in front of a flat table and were presented objects of five different shapes and dimensions. Objects shapes and dimensions are as follows: small circle (diam=3.2cm), small cube (l=9.5cm, w=3.2), big circle (diam=5.7cm), big cube (l=6.7cm, w=5.7cm), huge circle (diam=10 cm), and cylinder (diam=3.81 cm, height=10.8 cm). Wolf Motor Function Test (WMFT) [27] and Jebsen Test of Hand Function (JTHF) [28] measurements were taken for each subject prior to training and after training. The WMFT is a timed evaluation of upper extremity performance that measures limb and joint movement. The JTHF is a timed evaluation of hand function which simulates every day activities to measure fine motor and weighted hand functioning. Table 2.1 below lists subjects' clinical information.

**Table 2.1** Subject Clinical Information

| | Training | Level | Gender | Ataxia |
|---|---|---|---|---|
| SUBJECT 1 | VR | Moderate | F | N |
| SUBJECT 2 | VR | Moderate | M | N |
| SUBJECT 3 | VR | Moderate | M | Y |
| SUBJECT 4 | VR | Moderate | M | Y |
| SUBJECT 5 | VR | Severe | M | N |
| SUBJECT 6 | VR | Moderate | M | N |
| SUBJECT 7 | RTP | Mild | M | N |
| SUBJECT 8 | RTP | Mild | F | N |
| SUBJECT 9 | RTP | Mild | F | N |
| SUBJECT 10 | RTP | Severe | M | N |
| SUBJECT 11 | RTP | Moderate | M | N |

## 2.2 Data Capture

Position of joints and rotation of the subjects' arms were recorded using four electromagnetic sensors (trackSTAR™ system, Ascension Technologies, Inc.) attached with adhesive tape to the shoulder, elbow, wrist, and trunk. The trackSTAR™ (six degree of freedom) system's sensors output x, y, and z position coordinates of the magnetic center of the four sensors relative to the origin of the transmitter. Flexion and extension angles of finger joints were measured using resistive bend sensors in a glove (CyberGlove®, Immersion, Inc.) worn on both hands (Figure 2.1) [29].

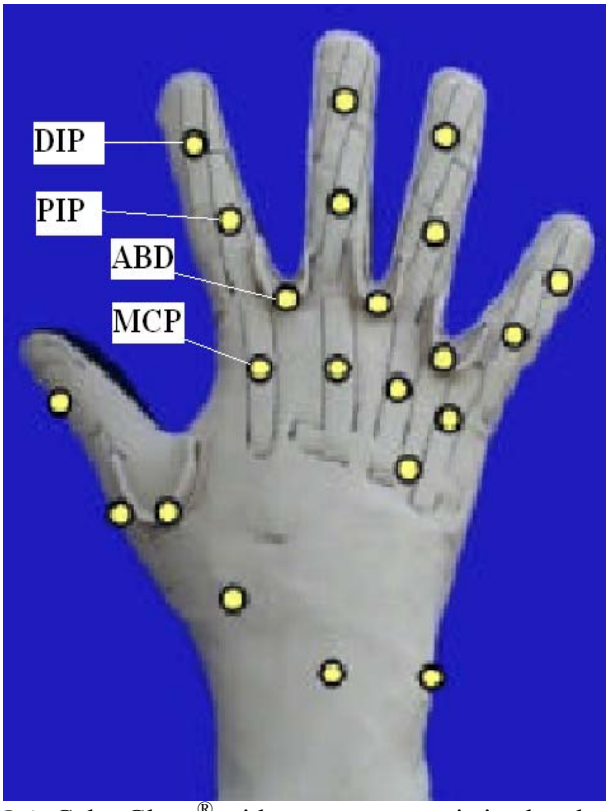


**Figure 2.1** CyberGlove® with twenty-two resistive bend sensors.

Source: Virtual Hand User's Guide. 2.7 [29]

The CyberGlove® sensors were individually calibrated for both hands for each subject during pre and post training sessions. Calibration measurements were obtained with hand position corresponding to zero degrees, 90 degrees, and 20 degrees by directing subjects to flatten their hand on a table with fingers together, make a fist, and keep hand flat on surface with fingers stretched apart respectively. Joint angles during experiments were calculated relative to their deviation from the zero, 90, and 20 degree calibration angles. The flexion/extension of the metacarpophalangeal (MCP), proximal interphalangeal (PIP), and distal interphalangeal (DIP) joints of all five fingers were included in this study as well as abduction/adduction (ABD) joints of all five fingers.

A six-axis force/torque sensor system (Nano17™, ATI Industrial Automation) was mounted below the object to measure vertical force exerted on the object (Figure 2.2). The 17 mm diameter transducer for this system converts the resulting force and torque into analog strain gage signals[30]. The force/torque controller converts strain gage data into force and torque data. These systems are connected to a PC through the serial port and all three devices were programmed using MATLAB and merged using C++. Devices were synchronized to capture data at 100Hz.

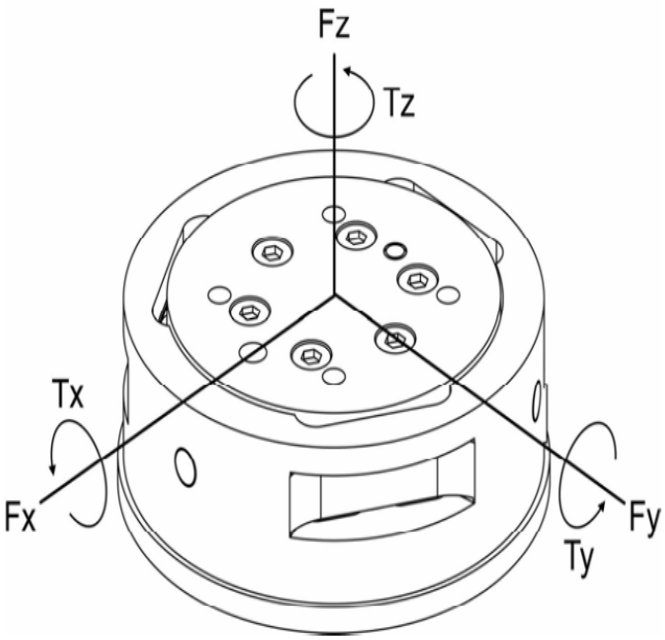


**Figure 2.2** Applied force and torque transducer.

Source: A. I. Automation, "F/T Controller (CTL/CTLJ/CON): Six- Axis Force/Torque Sensor System," p. 223, 2010. [30]

## 2.3 Procedure

At the beginning of each trial, the subject's hand is in a preset initial position. When cued, the subject is asked to reach to and grasp the object at a comfortable speed. Once the object is grasped, it is lifted by the subject and placed on a 7.5 cm high platform on the table surface (Figure 2.3). Trials were run for both impaired and unimpaired hands. Total trials per experiment were 120 (6 shapes x 2 hands x 10 trials). If an object was not grasped successfully, another trial was run to replace it.

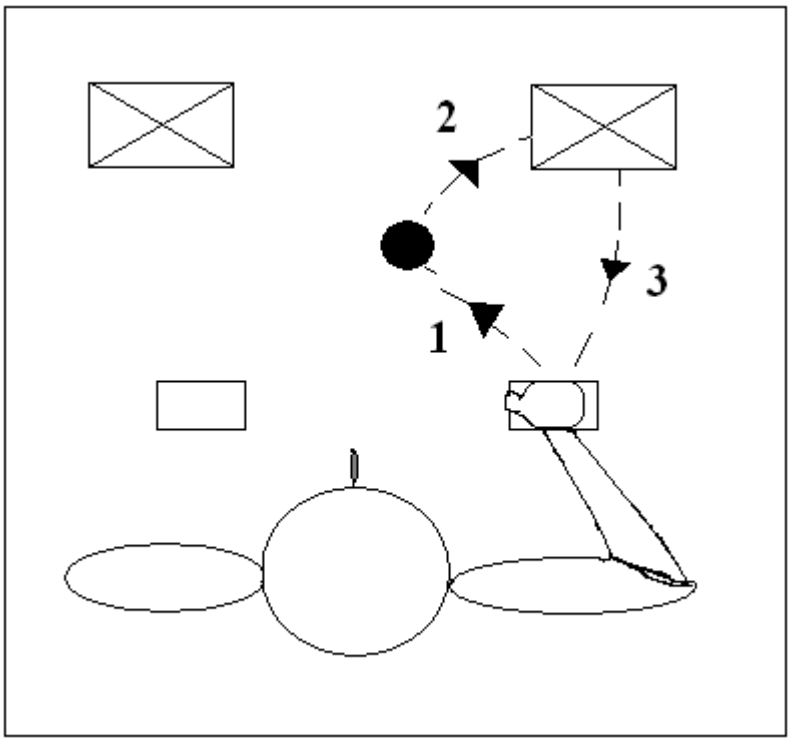


**Figure 2.3** Reach to grasp test schematic: Trial begins with hand at rest, placed in initial preset position. At cue, (1) subject reaches for the shape (centered) (2) places it on a 7.5 cm high target platform (3) returns to initial position. Trials are run for both hemiparetic and unimpaired hand**.**

## 2.4 Data Analysis

### 2.4.1 Nano17$^{TM}$

Data from the force sensor was validated using the position profile (Figure 2.4) from an electromagnetic sensor (trackSTAR$^{TM}$). Data retrieved from Nano17$^{TM}$ is organized into a matrix of six columns, the first three columns correspond to force components, $F_{x,}$ $F_{y,}$ $F_{z,}$ and the last three columns correspond to torque components, $T_{x,}$ $T_{y,}$ $T_{z.}$ The rows of the matrix correspond to the total number of samples which corresponds to total time of one

trial. To test the force sensor, one electromagnetic sensor was placed on the surface of the object 'big cube'. The force sensor was mounted below the object so that any displacement of the object would be detected by changes in force on the force sensor. A subject was seated in the typical reach to grasp experiment manner and when cued was asked to pick up the object and place it on a platform. Subject was not wearing a data glove and no electromagnetic sensors were attached to the subject for this force sensor test.

Figure 2.4 shows the z (vertical) position output from the electromagnetic sensor and the z directional force ($F_z$) output from the force sensor. Initially both profiles are constant with time, at approximately 1.61 seconds, the position graph dips below its initial position. This corresponds to the time the object was lifted. This data reveals that the time the object is lifted is 1.61 seconds for both the position and force graphs. This indicates that the time the hand reaches object is approximately 1.21 seconds and from 1.21 to 1.61 seconds, the subject is struggling to pick up the object (see force profile). From the position profile it can be inferred that between 1.61 seconds and approximately 4.21 seconds, the object is being transported from its initial position to the platform (final resting position).

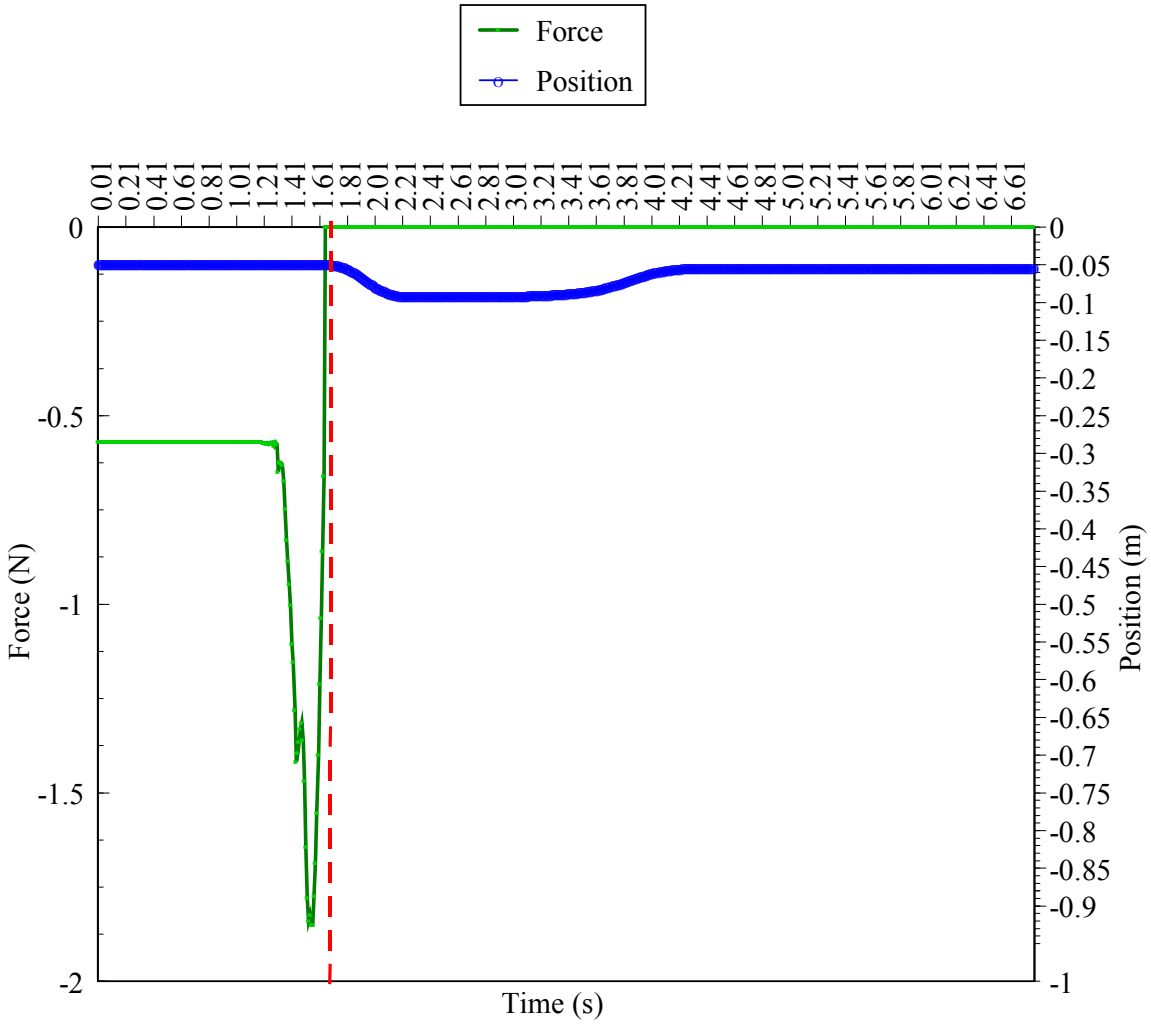


**Figure 2.4** Force and position graph.

Force data was further evaluated using velocity profiles obtained from the wrist position electromagnetic sensor during a reach to grasp experiment. The velocity profile in Figure 2.5 shows three peak velocities for the entire duration of a reach to grasp test. These peak velocities correspond to times of the three phases of movement: time of start to when hand reaches object, time when hand reaches object to when hand places object on platform, and time when hand places object on platform to when hand returns to initial position. The force profile shown below is plotted using data obtained from force $F_z$ component. The force profile shows a peak during the time when the hand applied

maximum force to the object during the first phase of movement. From approximately times 0-1.30 seconds, object is resting on force sensor, and from 1.96-3.75 seconds, there is no object on the force sensor because it has been lifted. Since data was acquired at 100 samples/second, maximum duration of movement is 3.75 seconds or 375 samples. Force sensor data was plotted with the velocity profile to confirm that the time during which the hand reaches object occurs in the same time period for both profiles. The force sensor data below indicates that from approximately 1.3 seconds to 1.96 seconds, the subject was struggling to lift the object. The time movement begins at approximately .6 seconds is referred to as onset1. The time hand reaches object is referred to as offset 1 (1.3 seconds) and the time hand lifts object is referred to has onset 2 (1.96 seconds).

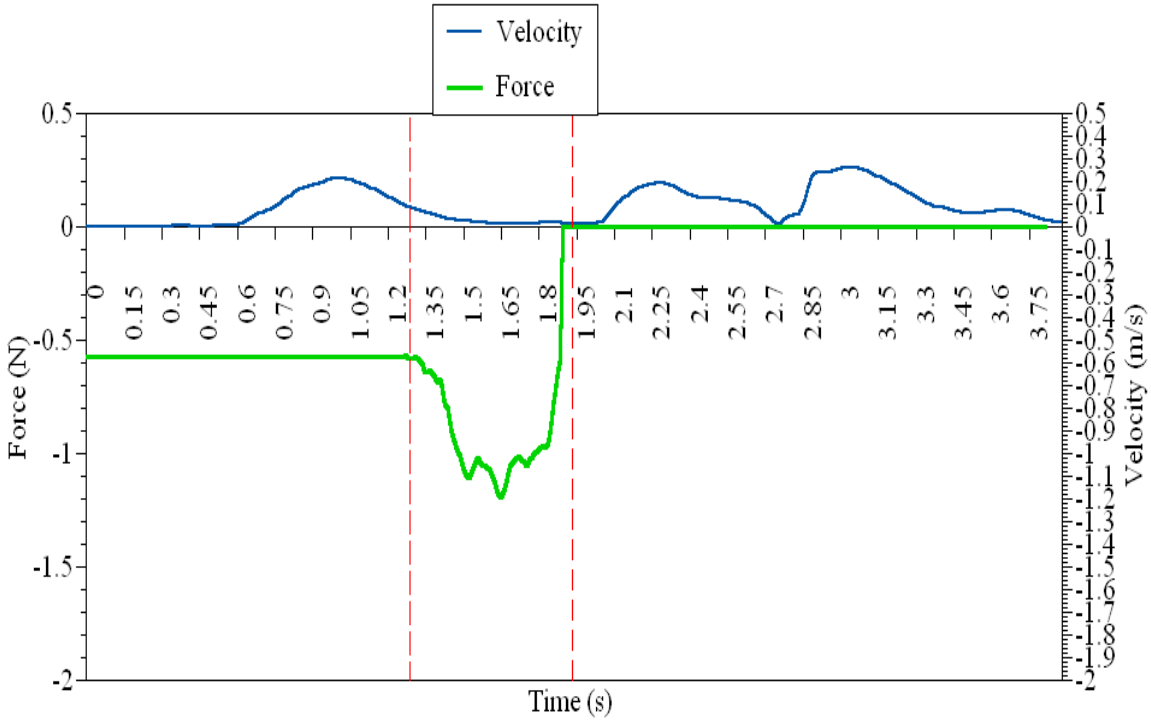


**Figure 2.5** Velocity and force profiles.

In order to determine the offset 1 and onset 2 times from the force sensor profiles, the raw force sensor data was smoothed by filtering with a 3rd order Butterworth digital low pass filter with a cutoff frequency of 5 Hz, which is well below the Nyquist sampling frequency. The butter function in Matlab was used to obtain the filter coefficients. Onset 2 and offset1 was determined by calculating the slope of the force profile. When the slope transitioned to a large negative value (-500), offset 1 was determined and when the slope transitioned to a low positive value (0.5), onset 2 was determined. For onset 2, a threshold was also applied so that under the condition of this threshold and low slope, onset 2 could be determined. Slope and threshold values were determined from trial and error of testing various force profiles for the six objects and six subjects. Maximum force applied to object was determined by compiling minimum force values from raw unfiltered data. Figure 2.6 is a flow chart that describes the steps in the MATLAB source code for determining offset 1 and onset 2 times. See Appendix A and Appendix B for full version of the source code.

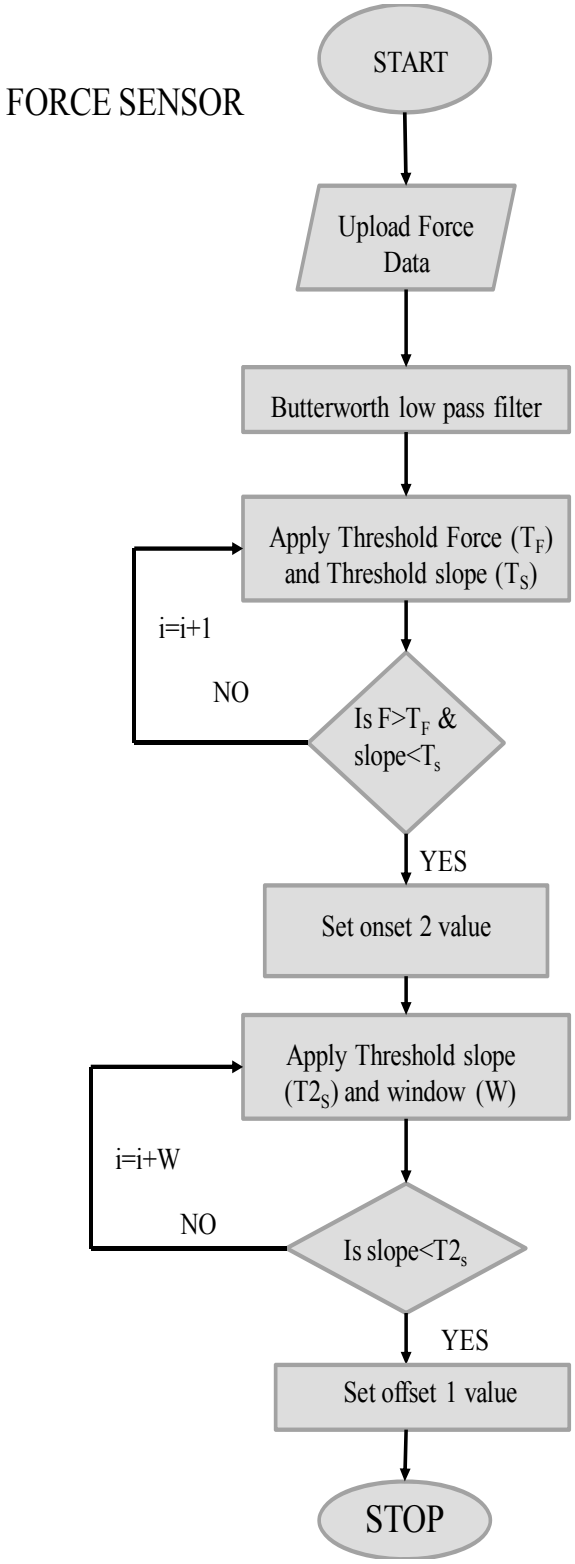


**Figure 2.6** Flow chart for MATLAB source code of force sensor data analysis.

### 2.4.2 Statistical Analysis of Kinematic and Force Data

The normal distribution is a probability model that describes the probability distribution of a continuous random variable (Figure 2.7). This model is generally bell-shaped where the center of the distribution refers to the highest probability. The x-axis are the values of the random variable X and the y-axis is the probability of observing that value of X where the total area under the curve is 1.0 [31].

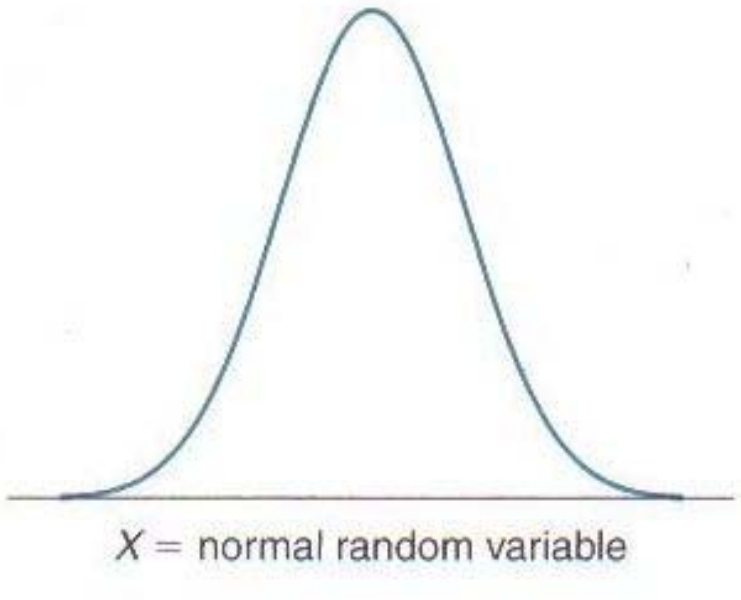


**Figure 2.7** The Normal Distribution.

Source: Ralph B. D' Agostino, S., Lisa M. Sullivan, Alexa S. Beiser (2006). Introductory Applied Biostatistics, Thomson Brooks/Cole. [31]

The mathematical formula for a normal probability distribution where x is a continuous random variable, μ is the mean of the random variable X, and σ is the standard deviation of the random variable is:

$$f(x) = \frac{1}{\sigma\sqrt{2\pi}} e^{-\left(-\frac{1}{2}\right)[(x-\mu)/\sigma]^2} \tag{2.1}$$

According to the Central Limit Theorem, taking random samples of size n with replacement from a population with mean μ and standard deviation σ, the sampling distribution of the sample means is normally distributed. This is generally true when n≥30, where $\mu_x$ is the mean of the sample means and $\sigma_x$ is the standard deviation of the sample standard deviations:

$$\mu_{x=}\mu, \quad \sigma_{x=}\frac{\sigma}{\sqrt{n}} \tag{2.2}$$

The Central Limit Theorem allows one to make inferences about the population based on the sample statistics $\bar{X}$. This inference is made by transforming to a standard normal distribution Z.

$$Z=\frac{\bar{X}-\mu_{\bar{X}}}{\sigma_{\bar{X}}} \tag{2.3}$$

However when the population standard deviation is unknown and the sample size is small (n<30), the Central Limit Theorem is not applicable and the distribution of the sample mean cannot be assumed as normal. For this case, the t-distribution is used which is similar to the standard normal distribution except in the tail end of the distribution. For small sample sizes (n<30) and an unknown population standard deviation (σ) a t-test is administered. A t-test is a statistical hypothesis test that follows a Student's t- distribution. The test statistic for paired data where $\bar{X}_d$ and $s_d$ are the mean and standard deviation of the difference scores and n is the number of pairs is:

$$t = \frac{\bar{X}_d - \mu_d}{\frac{s_d}{\sqrt{n}}} \quad (2.4)$$

For this study, a one-tailed paired Student's t-test was used to determine statistical significance of differences in time to reach object, grasping time, and maximum force applied to object pre training and post training. A paired t-test examines dependant samples, that is, a pre-treatment and post treatment. This study is one-tailed since the alternative hypothesis is that kinematic times post treatment have decreased and applied force has decreased. The null hypothesis is that the means are equal and the null hypothesis can be rejected when the p-value is less than α which in this case is .05. The p-value measures the significance of the data or the probability of observing a value that is as extreme or more extreme than the test statistic. Normality of distribution of data is verified by graphing a histogram of the data across several trials.

### 2.4.3 CyberGlove®

Data from CyberGlove® is stored in a matrix of twenty columns that correspond to twenty of the twenty-two joint angle sensors. Rows of the matrix correspond to total samples or total time of data collection. All raw glove data was 2nd order Butterworth low pass filtered with a cutoff frequency of 1 Hz to attenuate the high frequencies, and data was transformed from radians into degrees for analysis. Wrist trajectories and onset and offset times from force sensor data were used to determine a window of time for preshaping of the hand for each subject. Movement onset 1 is the time that movement first begins, offset 1 is the time the hand reaches the object, and onset 2 is the time of object lift. Onset 1 is measured as 5% of wrist peak velocity between onset 1 and offset

1. Figure 2.8 (not plotted to scale) is a kinematic profile of the entire movement sequence of the proximal interphalangeal joint for one trial beginning with initial resting position. The green trajectory is the joint angle profile of the index PIJ and the blue velocity profile was obtained by differentiating the position vector of the wrist sensor. Data collection begins after the subject is cued with the sound of a bell.

Phase 1 refers to the initial resting position upon hearing the bell. Phase 2 begins movement and corresponds to the reaching phase where hand preshapes to the object's shape. This is commonly referred to as the transport phase. As stated in previous literature, during the reaching phase, there is an acceleration, a peak velocity, and a deceleration [8]. Phase 3 begins when the hand reaches the object and the subject is struggling to pick up the object. Phase 4 begins with hand picking up object and transporting the object to the platform. Phase 5 refers to the time when the object is placed on the platform. Phase 6 refers to when the hand returns to the initial resting position. Phase 7 is the end of movement where hand is resting. The three peaks in the velocity profile correspond to the times in the movement when the hand is transported from the initial position to the object, from the object to the platform, and from the platform back to the initial position. The index PIJ trajectory reaches a minimum when it is grasping the object and returns to a value that is similar to the initial position (Phase 1) by the time it reaches Phase 7.

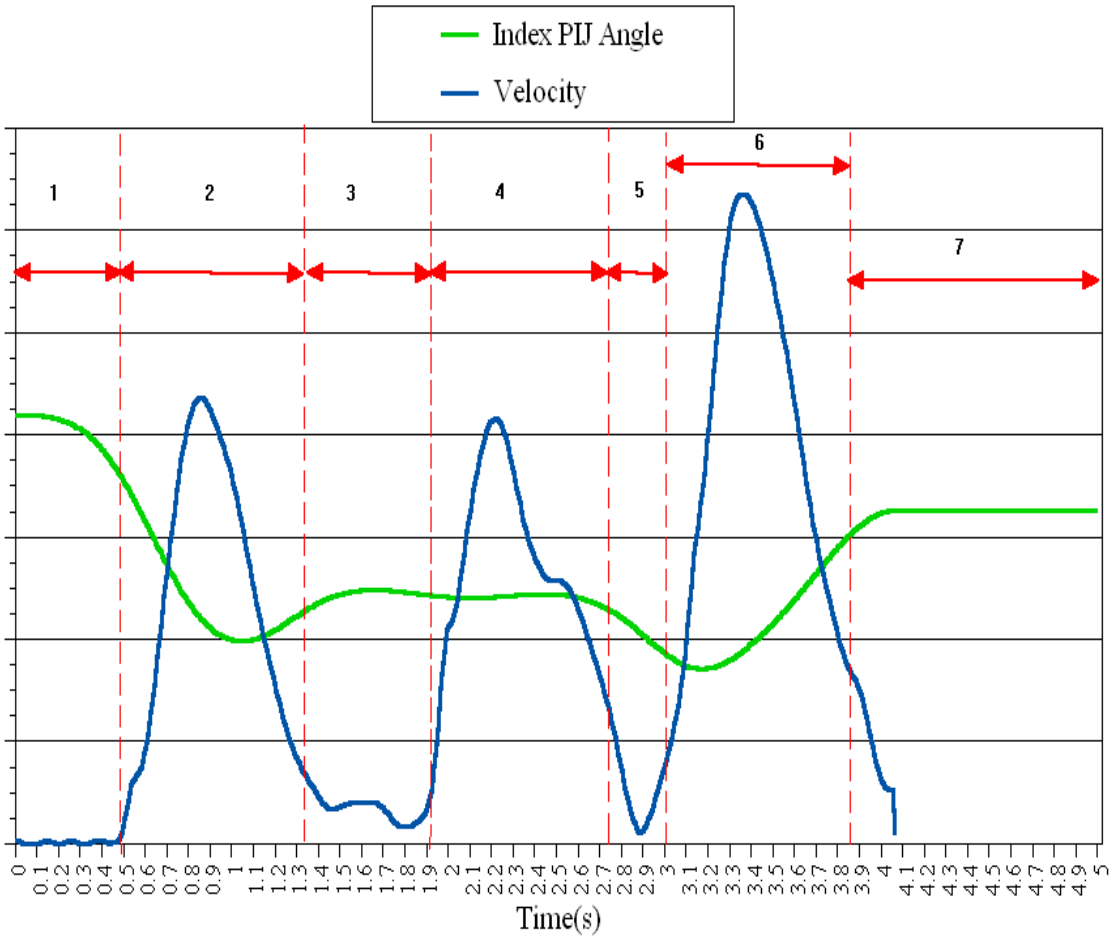


**Figure 2.8** Index PIJ joint angle sensor from CyberGlove® plotted with velocity profile from trakSTAR™ wrist sensor. Seven phases of movement are involved in the reach to grasp test. Duration of experiments varies for subjects depending on severity of impairment.

### 2.4.4 Classification of Hand Preshaping using Linear Discriminant Analysis

In statistics, machine learning, and pattern recognition, classification schemes are utilized to separate classes of data. Linear Discriminant Analysis (LDA) produces linear features which is beneficial for separating classes of multidimensional data (Figure 2.9). In this thesis, LDA is used in order to compare how accurately hand posture during the preshaping phase can predict what the target shape is pre and post rehabilitative training. In theory, LDA creates a decision boundary between different classes of

multidimensional data by projecting the data onto a new function which maximizes the ratio of between class scatter ($S_B$) or covariance between classes and within class scatter ($S_w$) or covariance within classes [32-34].

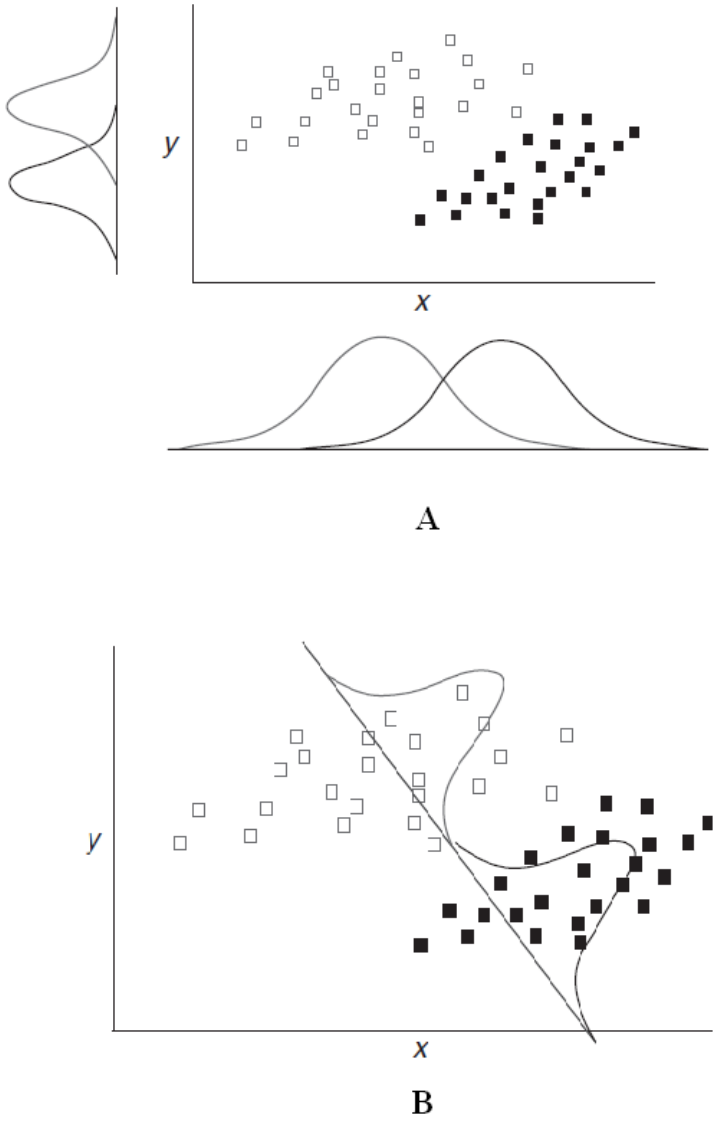


**Figure 2.9** LDA Class Separation: A shows the distribution for y-axis and x-axis projections. B shows the distribution using a new function formed from the linear combination of x and y.

Source: SPSS Discriminant Analysis**:** 589-604. [34]

The discriminant function (y) is computed by obtaining the eigenvector solution ($w^T$) for the ratio of $S_W^{-1}S_B$ where x is the multidimensional joint angle vector.

$$y=w^Tx \tag{2.5}$$

After transforming the hand postures into discriminant space, the minimum distance $D_{ij}^2$ between the hand posture and the mean of each class can determine which posture belongs to each class. In the present classification study, the training data, or the two classes are hand postures for two different shapes at one instant of time across multiple trials. The observation is classified into one of the two classes by calculating the Mahalanobis distances between the hand posture to be classified and the hand posture for each class where $S^{-1}$ is the pooled covariance matrix, where $x_i$ is a multidimensional observation, and $\mu_j$ is a multidimensional mean vector for the jth class.

$$D_{ij}^2 = (x_i-\mu_j)' S^{-1}(x_i-\mu_j) \tag{2.6}$$

The probability that a hand posture belongs to the jth class (G) given an observation vector X is determined by the posterior probability P(Gj|X):

$$P(Gj|X) = \frac{P(X|Gj)}{\sum_{j=1}^{k} P(X|Gj)} \tag{2.7}$$

P(X|Gj) is the probability that a hand posture in class j will have the observation vector X.

$$P(X|Gj) = f(X|Gj) = \frac{1}{\sqrt{(2\pi)^p\sqrt{|S|}}}\mathrm{e}^{(-1/2)\mathrm{Dij}^2} \quad (2.8)$$

The multivariate normal probability density function is $f(X|G_j)$. An observation is classified into one of two classes that has the minimum distance $D_{ij}^2$ or maximum posterior probability which is a function of $D_{ij}^2$. In order to compare hand postures using LDA, all movement data was synchronized such that onset 1 across trials occurred at the same time. Data captured during the reaching phase was normalized to 100 data points in order to concatenate the arrays across trials. The MATLAB function 'classify' was used to perform LDA analysis on the finger joint angles to obtain a measurement of error (misclassification) during the hand preshaping phase in predicting object shape.

LDA was performed for the preshaping phase, which is from times between onset 1 and offset 1 to predict which of the two objects the hand posture belonged to. Sensors measuring PIP, MCP, and abduction angles, of the index through ring fingers were analyzed to produce an eleven dimensional vector for two classes. Two matrices for each class were stacked to create a final matrix (m, n, j) where m is the samples, n is the 11 sensors for analysis, and j are the total number of trials for both objects. For every moment of time the posterior probability of one observation belonging to one of the two classes (groups) was calculated and the higher posterior was awarded the observation. Misclassification rate at every time point across trials was tabulated in order to report classification errors. Classification error was low pass filtered in order to produce the classification error curves. Figure 2.10 below is a flow chart of the LDA classification analysis for hand preshaping. See Appendix C and Appendix D for source code.

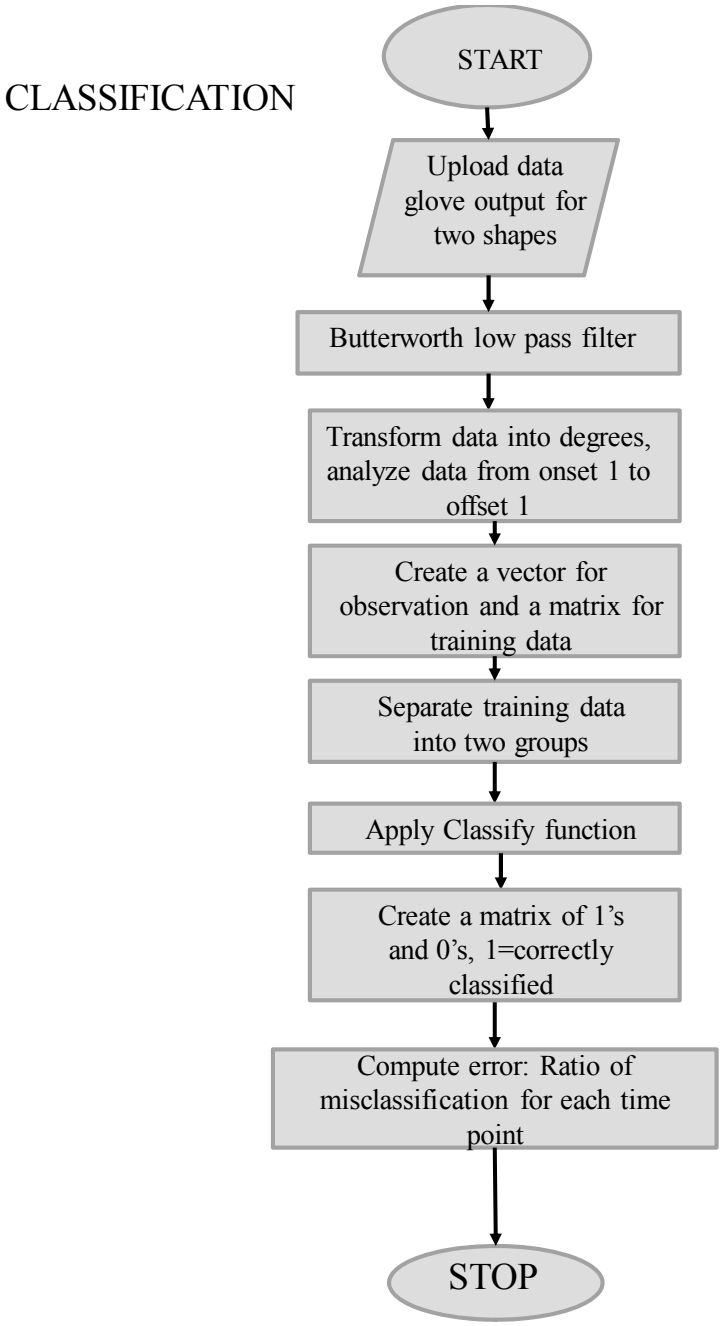


**Figure 2.10** Flow chart of MATLAB source code for classification of hand preshaping.

Figure 2.13 below shows a kinematic trajectory for both big cube and big circle of the unimpaired hand of Subject 9. This trajectory corresponds to the entire movement duration of a reach to grasp experiment. The red traces correspond to the subject reaching for the big cube object while the blue traces correspond to the big circle object. Joint angles for the big circle require greater extension and correspond to the lower angles when grasped since this hand formation is closer to the 0 degrees calibration position.

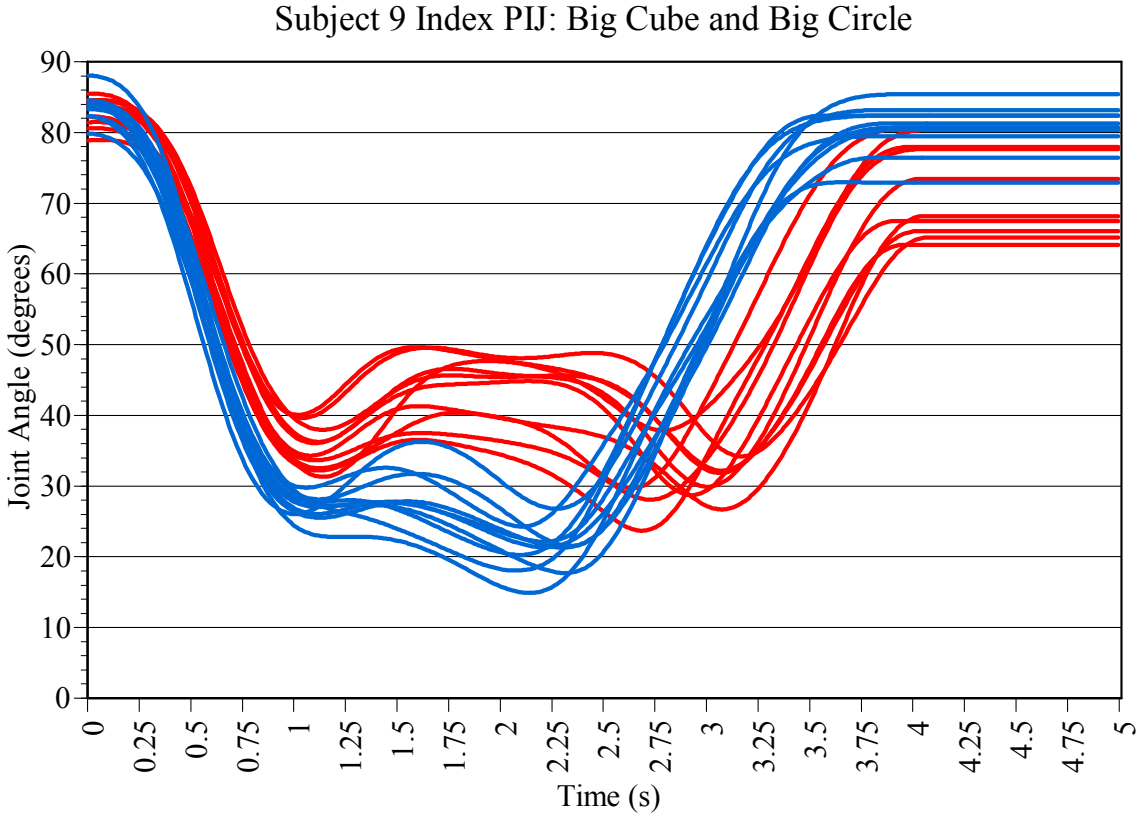


**Figure 2.11** Joint angle data for entire movement: big cube and big circle, 10 trials each.

Figure 2.12 below is identical to the trajectories in Figure 2.11 except that it considers only data from onset 1 to offset 1 and the data has been normalized to 100 samples. Figure 2.12 only considers movement in the preshaping phase (reaching).

From Figure 2.12 it can be seen that towards the end of movement, hand formation for big cube and big circle is completely distinguishable since the trajectories completely separate. Figure 2.12 shows how closely the hand postures for big circle and big cube resemble one another in the initial resting position until the end of movement where trajectories separate. For the LDA classification of hand posture for each subject, entire movement trajectories (Figure 2.11) were cut so that classification of hand preshaping was applied to only the hand formation phase (Figure 2.12). Figure 2.13 shows the resulting classification error of applying the LDA classification scheme to Figure 2.12.

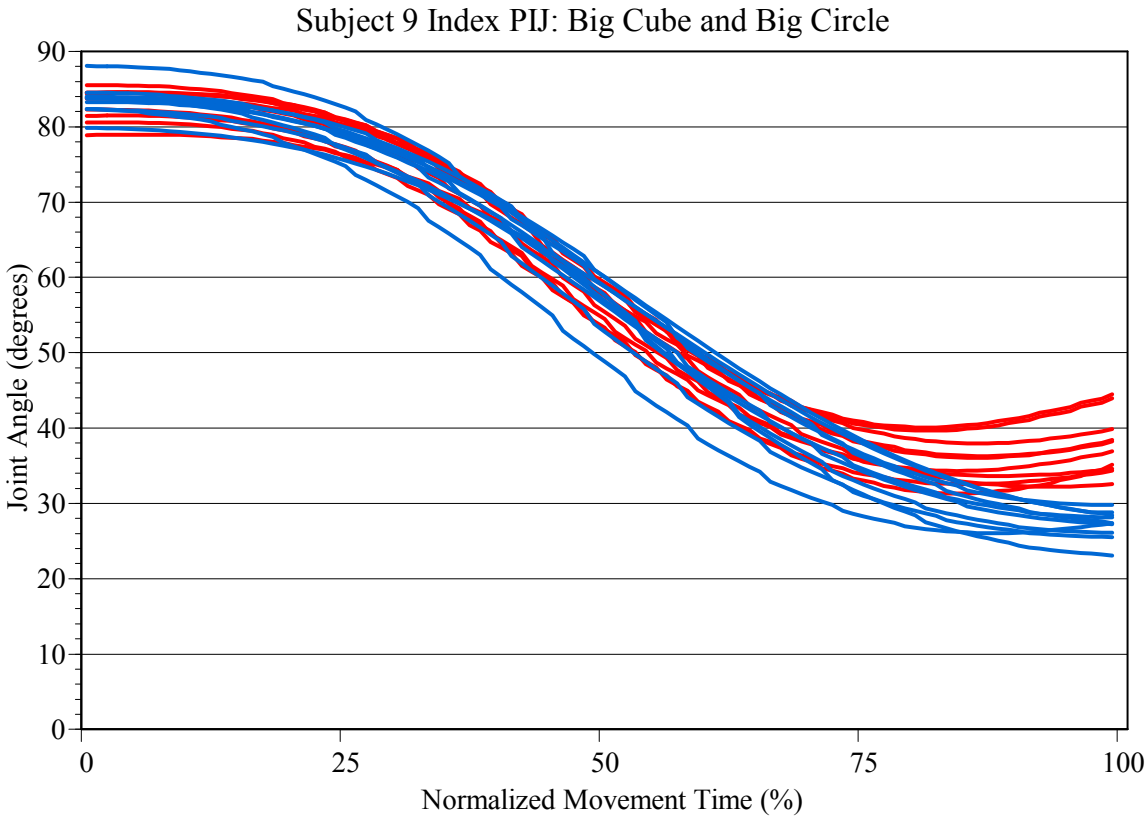


**Figure 2.12** Joint angle data for preshaping phase: big cube and big circle, 10 trials each, from onset1 to offset1.

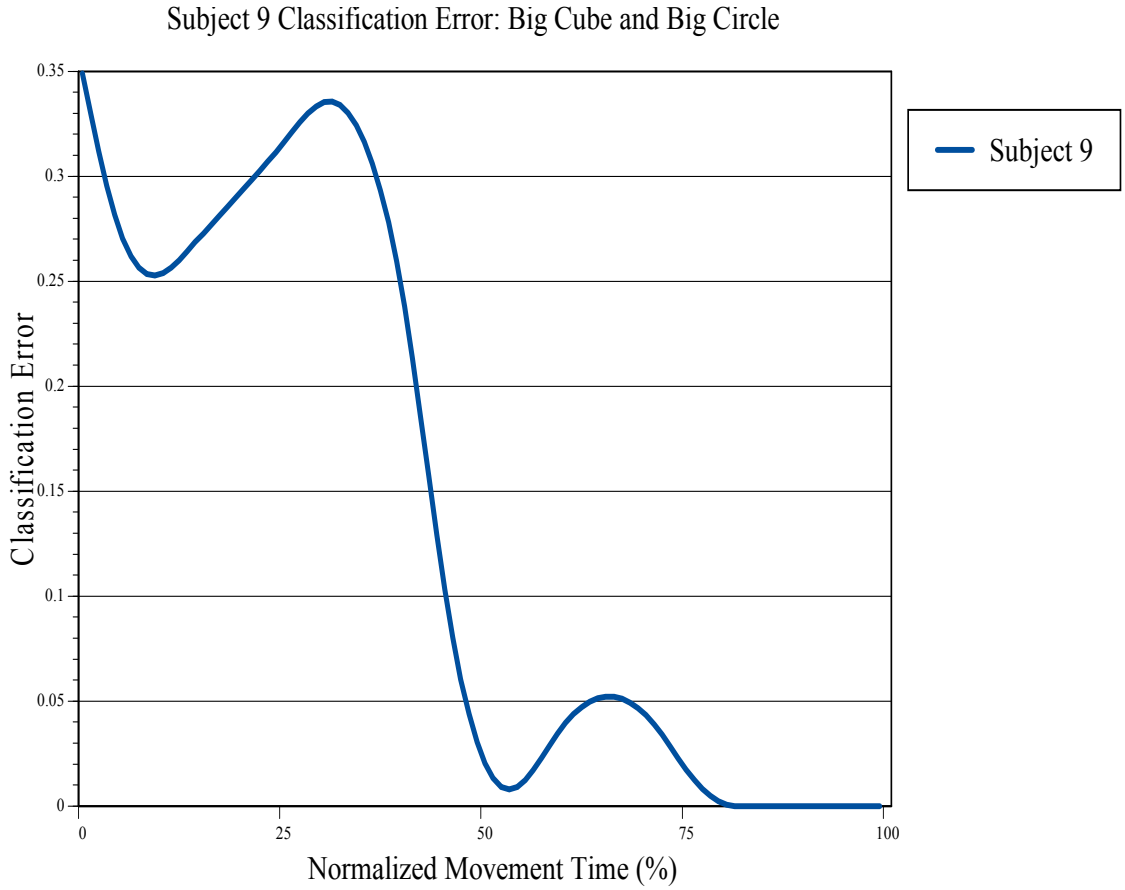


**Figure 2.13** Classification error of Figure 2.14. Error gradually decreases until the end of movement when error reaches zero.

### 2.4.5 Correlation of Finger Joint Angles

In order to investigate the dependences of finger joint angles, correlation coefficients (r) of finger joint angles between times onset 1 and offset 1 (hand preshaping phase) were calculated between combinations of MCP, PIP, and DIP joints of the index, middle, and ring fingers of the right data glove. Only the right data glove was analyzed since this glove has DIP sensors whereas the left data glove used in this study is exposed at the DIP joints. Glove data for subjects who were unimpaired in their right side were analyzed and compared to results from a previous study of correlations obtained during natural every day hand movements [35]. Where $\bar{x}$ is the mean of the first finger joint and $\bar{y}$ is the mean of the second finger joint for n measurements, the correlation coefficient is calculated as:

$$r = \frac{\sum_{i=1}^{n}(x_i-\bar{x})(y_i-\bar{y})}{\sqrt{\sum_{i=1}^{n}(x_i-\bar{x})^2 \sum_{i=1}^{n}(y_i-\bar{y})^2}} \tag{2.9}$$

Correlation values vary between -1 and 1. A value of 1 implies perfect linear relationship between the two variables such that an increase in the first variable dictates an increase in the second variable. A value of -1 implies a negative linear relationship between the two variables such that an increase in the first variable dictates a decrease in the second variable. A value of zero implies no relationship.

# CHAPTER 3

# RESULTS

## 3.1 Total Movement Time: Hemiparetic

Total movement time (MT) is the time from onset of movement (onset1) to when the hand reaches object (offset1). All subjects in the RTP group decreased their average MT post training (Table 3.1). Three out of five RTP subjects show a statistically significant ($p<.05$) decrease in MT (asterisk for subjects with significant improvement). In the VR training group, four out of six subjects decreased their total movement time post training. Subjects 2 and 5 increased their MT post training. One subject in the VR training group showed statistically significant decrease in MT. Group mean MT for both VR trained and RTP trained show the impaired hand's MT is greater than that of the unimpaired hand's MT (Figure 3.1, Figure 3.2). For both groups, shapes 1, 2, 3, and 4, correspond to 'small circle', 'small cube', 'big circle', and 'big cube' respectively. For the VR group shape 5 corresponds to the shape 'huge circle' and for the RTP group shape 5 corresponds to the shape 'cylinder'. As a group, RTP subjects' MT was greatest for 'cylinder' for both hands. There were no consistent trends in MT's for the VR group that is based on object shape.

**Table 3.1** Total Movement Times

| | Pre Training (s) | Post Training (s) | Training |
|---|---|---|---|
| SUBJECT 1 | 1.30 | 1.05 | VR |
| SUBJECT 2 | **0.72** | **0.85** | VR |
| SUBJECT 3 | 1.31 | 1.16 | VR |
| SUBJECT 4* | 1.17 | 0.96 | VR |
| SUBJECT 5* | **0.65** | **0.76** | VR |
| SUBJECT 6 | 1.41 | 1.41 | VR |
| SUBJECT 7* | 0.84 | 0.69 | RTP |
| SUBJECT 8* | 0.57 | 0.40 | RTP |
| SUBJECT 9* | 0.71 | 0.59 | RTP |
| SUBJECT 10 | 2.29 | 2.41 | RTP |
| SUBJECT 11 | 1.29 | 1.20 | RTP |

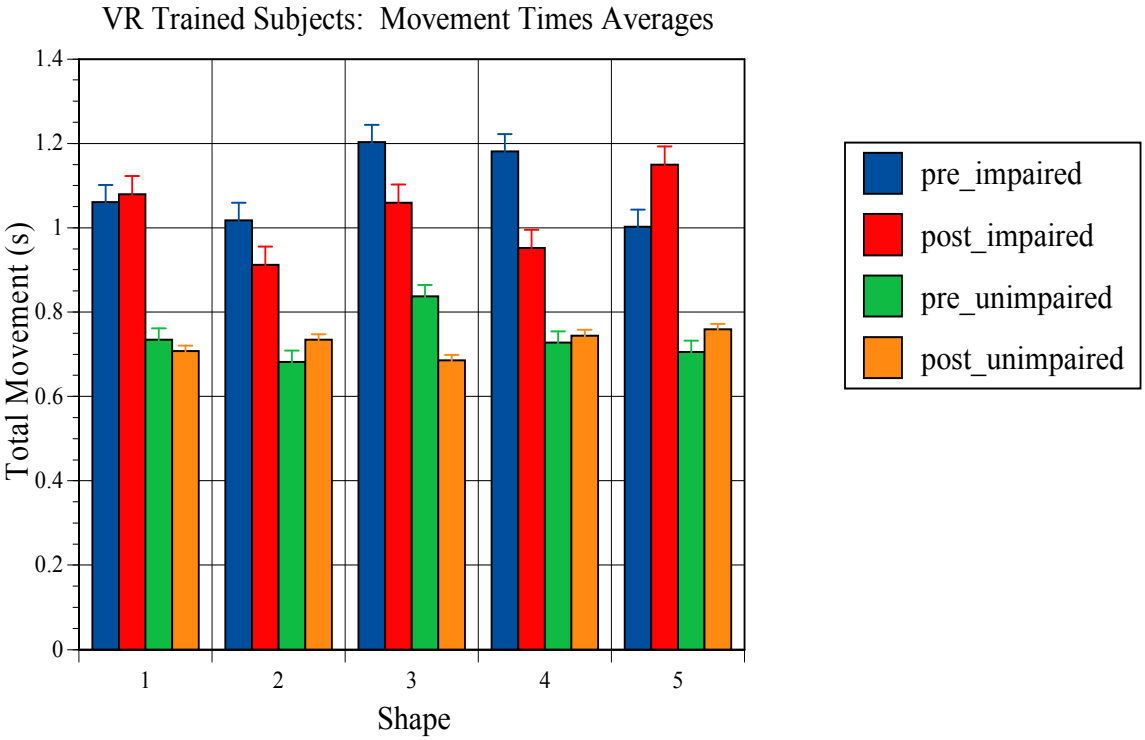


**Figure 3.1** Group movement time averages for VR training.

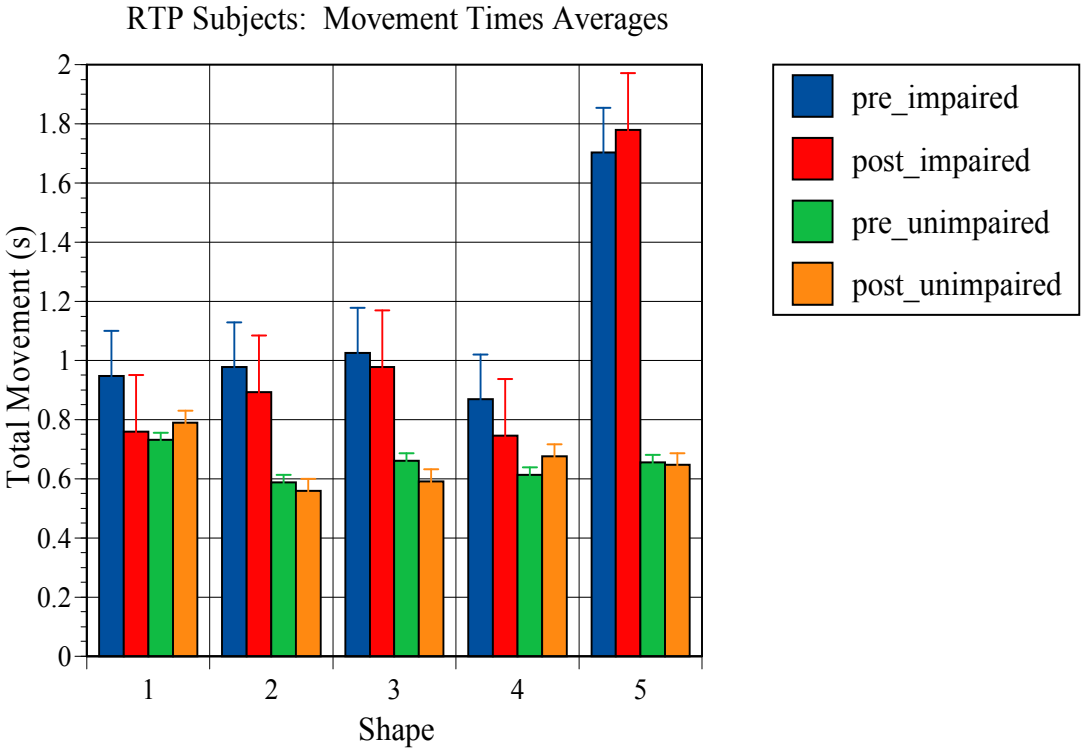


**Figure 3.2** Group movement time averages for RTP training.

## 3.2 Total Grasping Times (Hemiparetic)

Grasping time is measured as the time period in which hand touches object and picks it up (Phase 3 in Figure 2.8 above). Three out of six subjects in the VR training group decreased their grasping time post training (Table 3.2). All five subjects in the RTP group decreased their grasping time post training with statistically significant ($p<.05$) decreases for four subjects. Subjects with an asterisk corresponds to a significant p-value and values in bold correspond to an increase in MT.

**Table 3.2** Group Grasping Times

| | Pre Training (s) | Post Training (s) | Training |
|---|---|---|---|
| SUBJECT 1 | 1.58 | 1.39 | VR |
| SUBJECT 2 | **0.34** | **0.39** | VR |
| SUBJECT 3 | 0.12 | 0.09 | VR |
| SUBJECT 4* | **0.53** | **0.72** | VR |
| SUBJECT 5 | 0.95 | 0.80 | VR |
| SUBJECT 6 | **1.52** | **1.55** | VR |
| SUBJECT 7* | 0.15 | 0.09 | RTP |
| SUBJECT 8* | 0.20 | 0.12 | RTP |
| SUBJECT 9* | 0.40 | 0.25 | RTP |
| SUBJECT 10* | 0.25 | 0.12 | RTP |
| SUBJECT 11 | 0.50 | 0.44 | RTP |

## 3.3 Force Sensor

Force sensor data for average maximum force applied to the object by the VR subjects pre and post training shows a statistically significant ($p<.05$) decrease in average force applied to objects for three out of five subjects for a majority of objects (Table 3.3). Average force difference is the difference in vertical force between pre training and post training. Negative values correspond to an increase in force post training. For subjects 5 and 6, average force applied to object increased post training, where statistical significance is only seen for two objects. Values with an asterisk correspond to a significant p-value and negative values correspond to an increase in force applied post training.

**Table 3.3** Average Force Difference (N)

| | Big Circle | Big Cube | Huge Circle | Small Circle | Small Cube |
|---|---|---|---|---|---|
| SUBJECT 1 | 0.51* | 0.36* | -1.80 | 0.04* | -0.19* |
| SUBJECT 2 | 0.32* | 0.61* | 0.27* | 0.03* | 0.10 |
| SUBJECT 4 | 0.78* | 0.47* | 0.34 | 0.09* | -0.86* |
| SUBJECT 5 | -1.33 | -0.21 | -0.26 | -0.10 | -0.37* |
| SUBJECT 6 | -2.81 | 0.17* | -0.41 | -0.06 | -0.48 |

## 3.4 LDA Classification of Hand Preshaping

Finger joint angle analysis from all eight subjects show a decrease in error post VR training and RTP training indicating that discriminating hand shape during prehension for the subjects improved. Table 3.4 presents the times at which subjects reached an error of zero (times are normalized to percent of movement). An error of zero implies accurate hand preshaping for the target object and the ability of the classifier to distinguish between two objects' hand postures. In Table 3.4, all subjects reached an error of zero earlier in time post-training than pre-training. Three subjects did not reach an error of zero until after the hand touched object; Subject 3, Subject 4, and Subject 5.

Table 3.5 presents classification errors for these three subjects throughout the duration of their movement. In post-training, the three subjects achieve lower classification errors than pre-training throughout their movement. Subject 3 and Subject 5 do not reach an error of zero when hand touches object. Figures 3.3, 3.4, and 3.5 shows typical profiles of classification errors in prediction object shapes. As expected, the unimpaired hands present lower classification errors than the impaired hand. Subject 1's error rate for "huge circle" and "small circle" for both impaired hand and unimpaired hand decreases after training. After 75% of the transport phase, both hands produce distinguishable hand shapes for these objects. Figure 3.4 presents Subject 9's classification errors also indicate distinguishable hand posture and high accuracy in hand preshaping by 75% of the preshaping phase. Figure 3.5 presents the classification errors of the impaired hands of two subjects pre and post training. Classification errors for the severely impaired subject is greater than that of the mildly impaired subject even after

50% of movement duration. Both subjects show an improvement in preshaping accuracy post training.

**Table 3.4** Times of Minimum Classification Error

| Minimum Classification Error of Hemiparetic Hand: Normalized Movement Time(%) | | |
|---|---|---|
| | Pre-Training | Post-Training |
| SUBJECT 1 | 74% | 58% |
| SUBJECT 3 | **100%** | **100%** |
| SUBJECT 4 | **100%** | **100%** |
| SUBJECT 5 | **100%** | **100%** |
| SUBJECT 7 | 60% | 32% |
| SUBJECT 8 | 72% | 47% |
| SUBJECT 9 | 64% | 55% |
| SUBJECT 11 | 100% | 71% |

**Table 3.5** Classification Errors as Movement Progresses

| Classification Errors of Hemiparetic Hand: Normalized Movement Time (%) | | | | | | | | | |
|---|---|---|---|---|---|---|---|---|---|
| | Pre-Training | | | | | Post-Training | | | |
| | 25% | 50% | 75% | 100% | | 25% | 50% | 75% | 100% |
| SUBJECT 3 | 0.22 | 0.09 | 0.25 | 0.10 | | 0.21 | 0.09 | 0.19 | 0.05 |
| SUBJECT 4 | 0.31 | 0.31 | 0.21 | 0.00 | | 0.21 | 0.10 | 0.14 | 0.00 |
| SUBJECT 5 | 0.12 | 0.38 | 0.26 | 0.16 | | 0.22 | 0.23 | 0.18 | 0.06 |

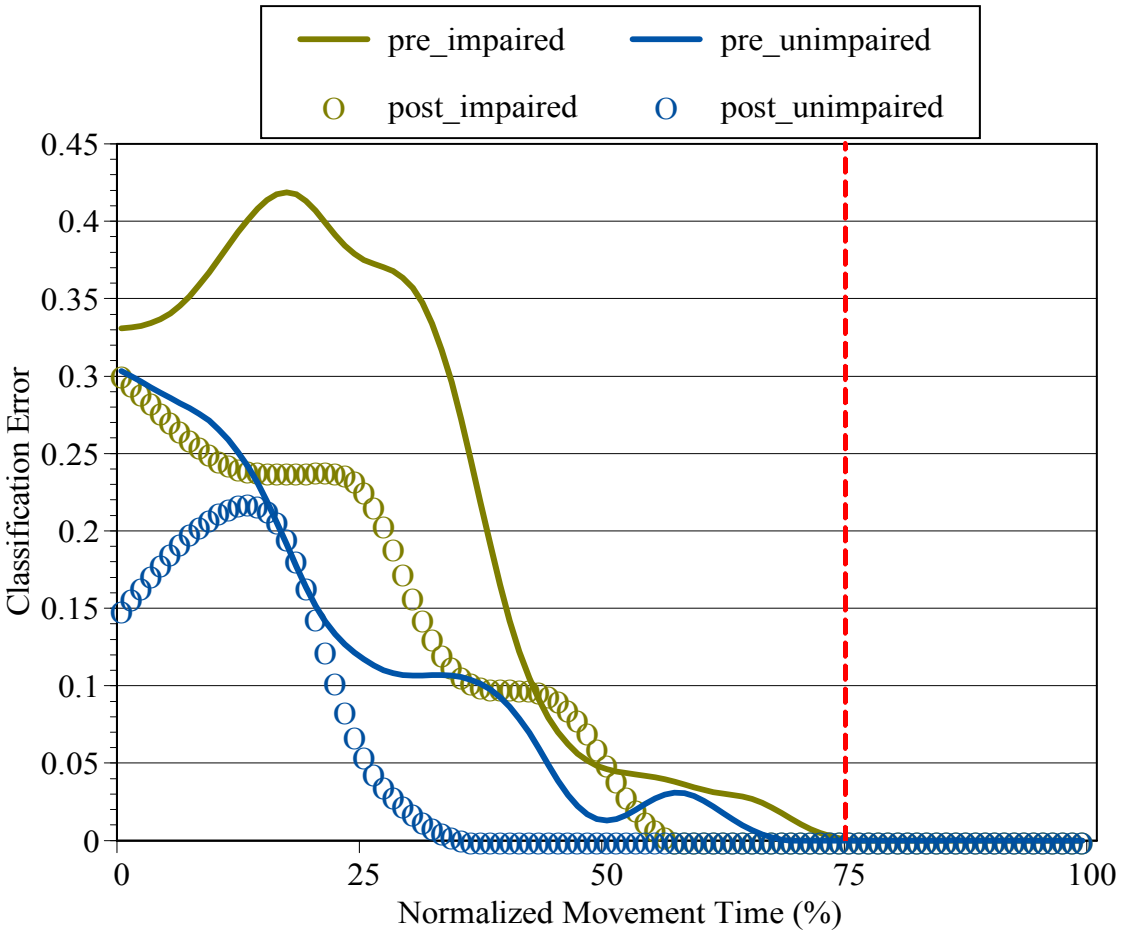


**Figure 3.3** Subject 1 classification errors of huge circle and small circle. Subject 1 was VR trained.

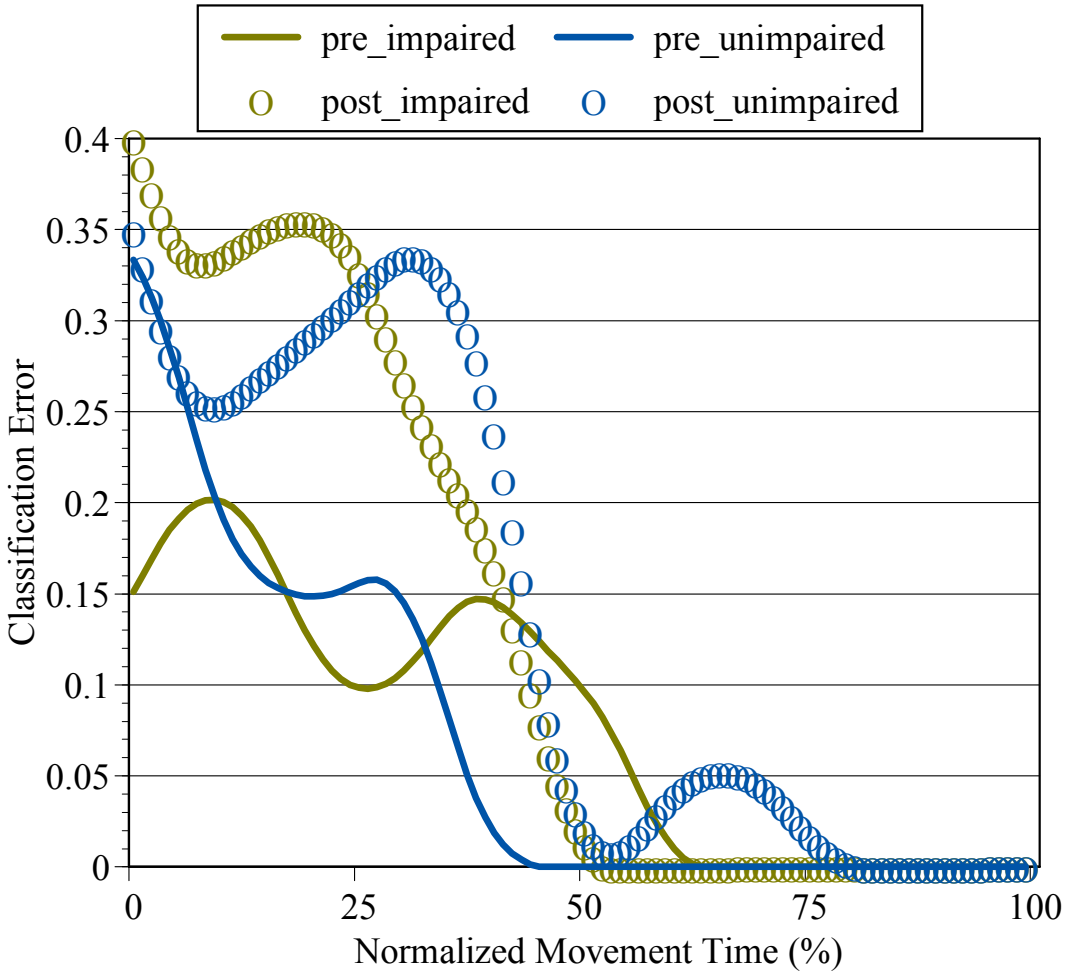


**Figure 3.4** Subject 9 hemiparetic hand classification error for cylinder and small cube. Subject 9 is a mildly impaired subject and is RTP trained

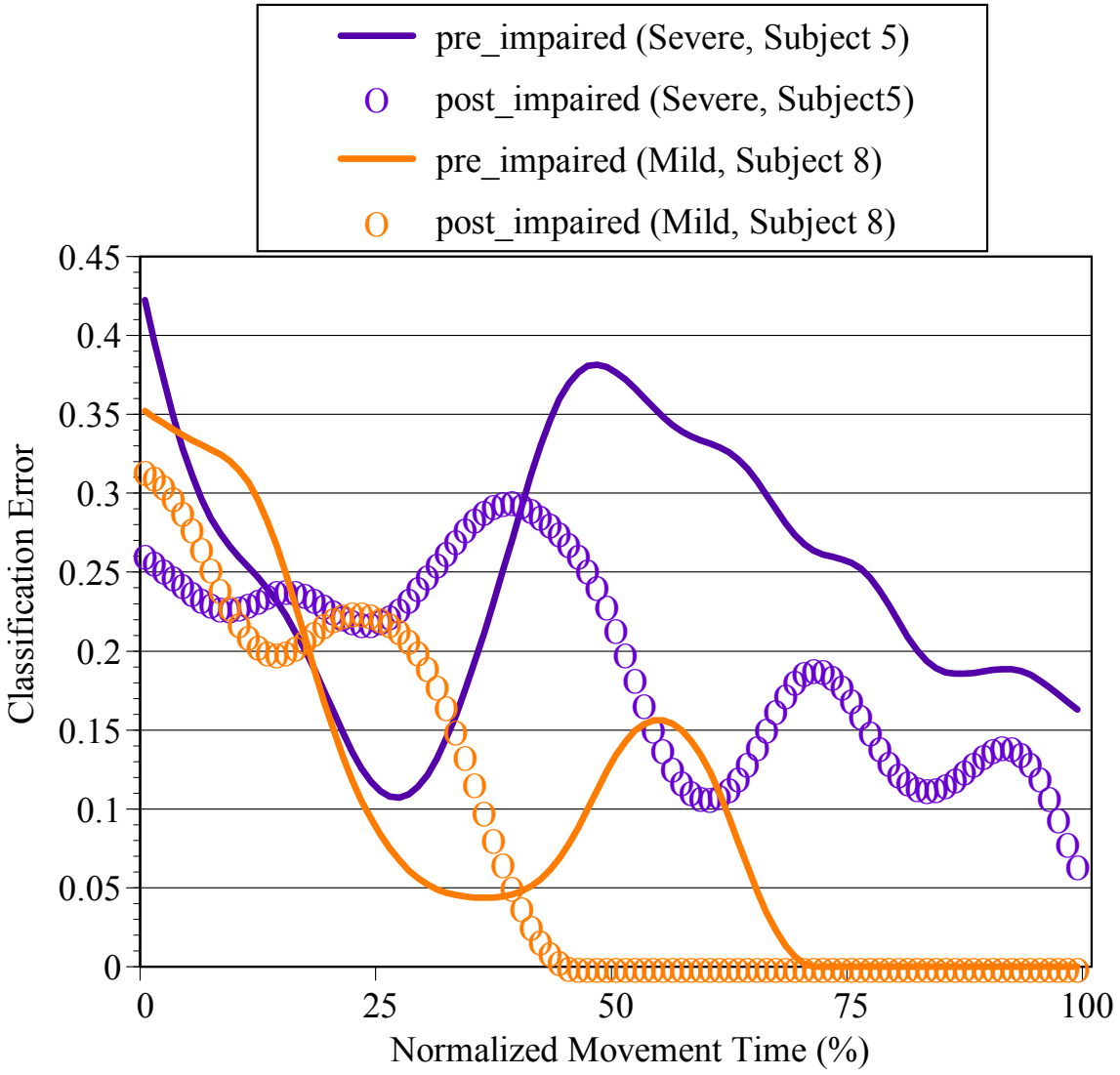


**Figure 3.5** Classification error of hemiparetic hand for severe and mild impairment: Subject 5 is VR trained and Subject 8 is RTP trained. Both subjects show improvement in hand preshaping post training.

### 3.5 Correlation of Finger Joint Angles

Figure 3.6 presents the average correlations between three different pairs of joints of the same finger during a reaching task. Average MCP-PIP and MCP-DIP correlations for the index, middle, and ring finger indicate a negative correlation when preshaping fingers for shapes big circle, big cube, small circle, and small cube. However, PIP-DIP joint pair averages indicated a positive correlation. Figure 3.7 presents average correlations for each joint across fingers. During reaching, correlations of pairs of index, middle, and ring fingers show that PIP has the highest average correlation while DIP has the weakest correlation. Figure 3.8 presents the correlations of each joint with respect to distance. For each joint, correlations of index to middle finger (0 finger separation), middle to ring finger (0 finger separation) and index to ring finger (1 finger separation) were computed. Results show that correlations for each joint decreases with increasing finger separation.

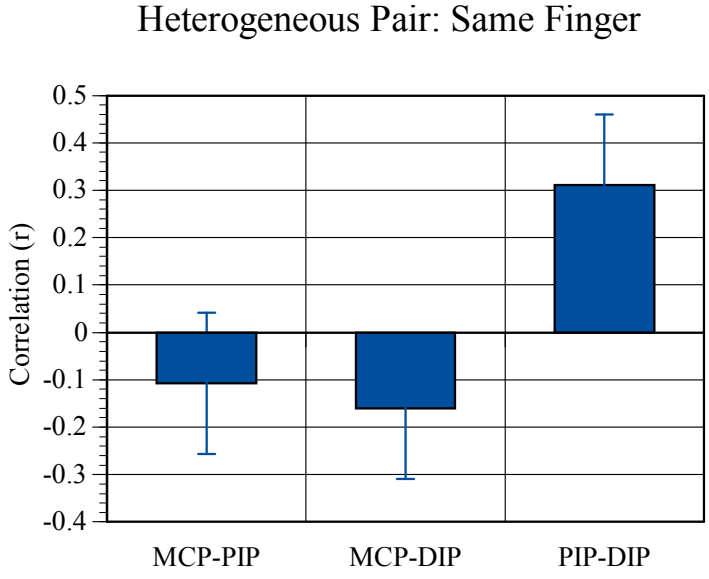


**Figure 3.6** Average correlations for joint angle pairs of the same finger in a reaching task

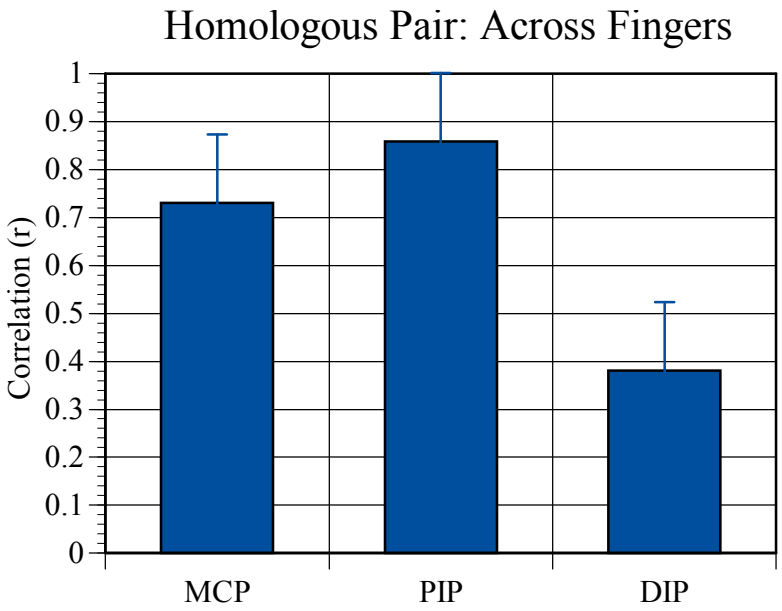


**Figure 3.7** Average correlations across fingers for pairs of same joints

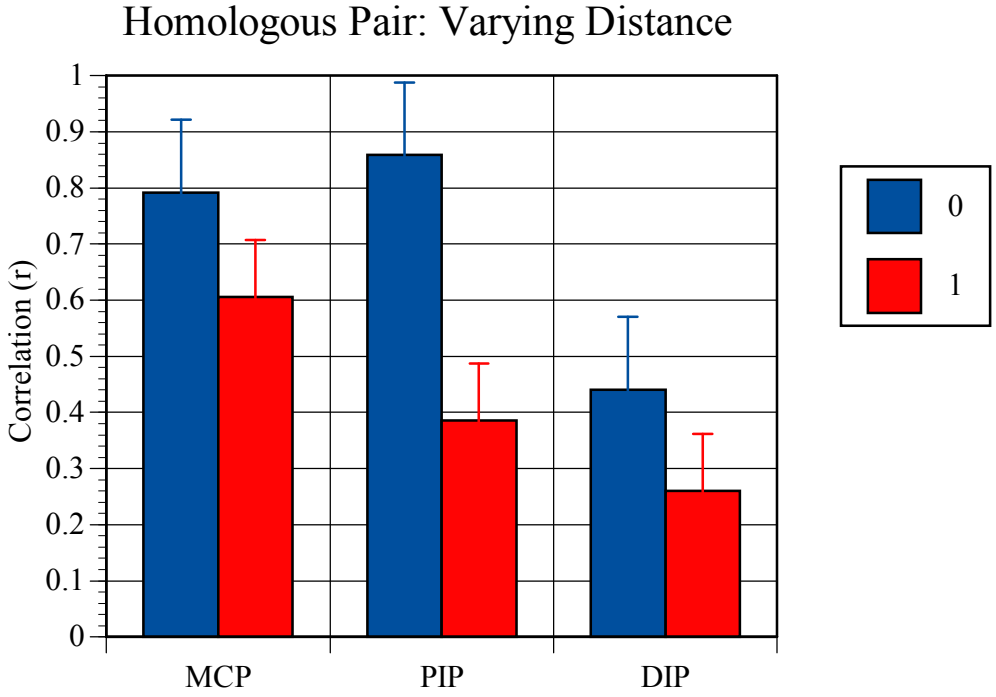


**Figure 3.8** Average correlations for varying finger separation

# CHAPTER 4

# DISCUSSION

A decrease in total movement time post training is in line with results from previous studies of subjects who are VR trained and trained with conventional physical therapy. A decrease in average total movement time to target object and average grasping time of target object suggests that post training, patients were able to move and grasp more efficiently and accurately during the reach to grasp test. On average, subjects in the RTP group had highest movement times when reaching for the 'cylinder', which is the largest sized object for that group. If the 'cylinder' object was available in the VR group, perhaps similar results could be observed.

The decrease in applied force during grasping can be due to increased control of the hemiparetic arm and hand following VR training which allows the subject to press down on the object with less intensity. According to the Wolf Motor Function Test, Subject 5 and Subject 6 are the most impaired subjects. This may explain the subjects' deviation in applied force measurements post training compared to Subject 1, 2, and 4. These results are similar to a previous study that showed that enhanced physical therapy did not show improvement for subjects who were severely impaired [21]. As indicated by this thesis, the use of a force sensor is beneficial in reach to grasp tests since it provides an accurate representation of the grasping phase, force applied, and a reliable determination for offset 1 and onset 2 times (grasping times).

Correlations of finger joint angles during the reaching phase show the dependence of finger joint angles. Results from this study are similar to that of previous research

which show strongest correlations between PIP-DIP joints and weakest correlations between MCP-PIP and MCP-DIP joints [35]. However in this study, MCP-PIP and MCP-DIP present a weak negative correlation. Similar to previous research, homologous joint pairs of DIP joints exhibit the weakest correlation between fingers. Also, with increasing finger separation, the correlation between homologous joint pairs decreases. That is, the correlation between MCP joints of the index/middle fingers and middle/ring fingers are higher than that of the index and ring fingers. This relationship of decreasing correlation with increased finger distance is consistent for joint pairs of the MCP, PIP, and DIP joints.

As a group, subjects tend to begin with larger classification error rates since during the resting position finger joint angles show little differences between objects, and minimum error rates at the end of movement since object has been grasped to form the contours of the shape. As expected, classification errors for the impaired hand tend to be much higher than that of the unimpaired hand since hemiparesis hinders fine finger movement. The results of this study are in line with previous research which indicates that low classification errors can be attained before 50% of movement [12]. As expected, Subject 3, 4, and 5 who did not achieve zero classification errors at 100% of movement correspond to subjects who had higher levels of motor difficulty. Subjects 3 and 4 are ataxic and Subject 5 is the most clinically impaired subject in the study. For all subjects, when movement begins (transport), the hand gradually evolves in order to optimize hand formation for the target shape [11].

Improvement in classification errors or decrease in error during post training sessions may indicate improvement in fine finger movement. Since the classification

error results consider up to eleven finger joint angles from the index to ring fingers, this analysis may provide insight into improvement in finger fractionation (finger independence) [26]. Since reaching and grasping involve different neural mechanisms, patients with neurological difficulty such as stroke subjects may be able to reach efficiently but have difficulty grasping and vice versa [19]. However, since these movements are synchronized, many patients experience difficulty in both types of motor control.

Figure 2.11 demonstrates a smooth and consistent joint angle trajectory of one subject's unimpaired hand. In a majority of stroke subjects however, this trajectory is a stark contrast to the hemiparetic hand trajectory which shows disruptions in coordination and an inability to maintain stability. It is this variance in the trajectory of the joint angles of the hemiparetic hand that is observed to have varied post treatment. Since stroke subjects have difficulty controlling individual finger movements and coordination, improvements in motor control post treatment can be observed in trajectories that closely approximate the mean for each object being grasped. This tighter trajectory can be a measure of accuracy regarding optimizing hand formation. Across multiple trials, trajectories with lower variance seem to imply an ability to preshape with greater accuracy. The classification scheme presented in this study is intended to measure the variability of the trajectories post training versus pre training and how treatment affects the predictability of hand preshaping.

# CHAPTER 6

# CONCLUSION

Virtual reality training of the hemiparetic arm and hand and conventional physical therapy can improve stroke subjects' abilities to reach for objects and grasp them. Due to the variety of subject demographics and severity of impairments, as well as the individual rehabilitative treatment of each subject, it is difficult to quantify improvement in subjects' reaching and grasping abilities. However, the present study demonstrates that these therapies are equally beneficial in aiding rehabilitation of subjects with hemiparesis. Virtual reality training with assistive robotics is particularly useful in quantifying motor treatments and providing an individualized and interactive training environment. Post treatment, subjects exhibit lower movement times and grasping times as well as a decreased use of force. Classification of hand preshaping is a predictive model that shows improved accuracy in predicting object shape following training. Classification results demonstrate that training promotes fine movement of fingers in subjects. The system as described utilizing magnetic trackers, a data glove, and a force sensor is sensitive to changes in motor performance following a virtually simulated motor intervention and conventional physical therapy.

# APPENDIX A

## CHAPTER 3 ADDITIONAL FIGURES FOR CLASSIFICATION OF HEMIPARETIC HAND

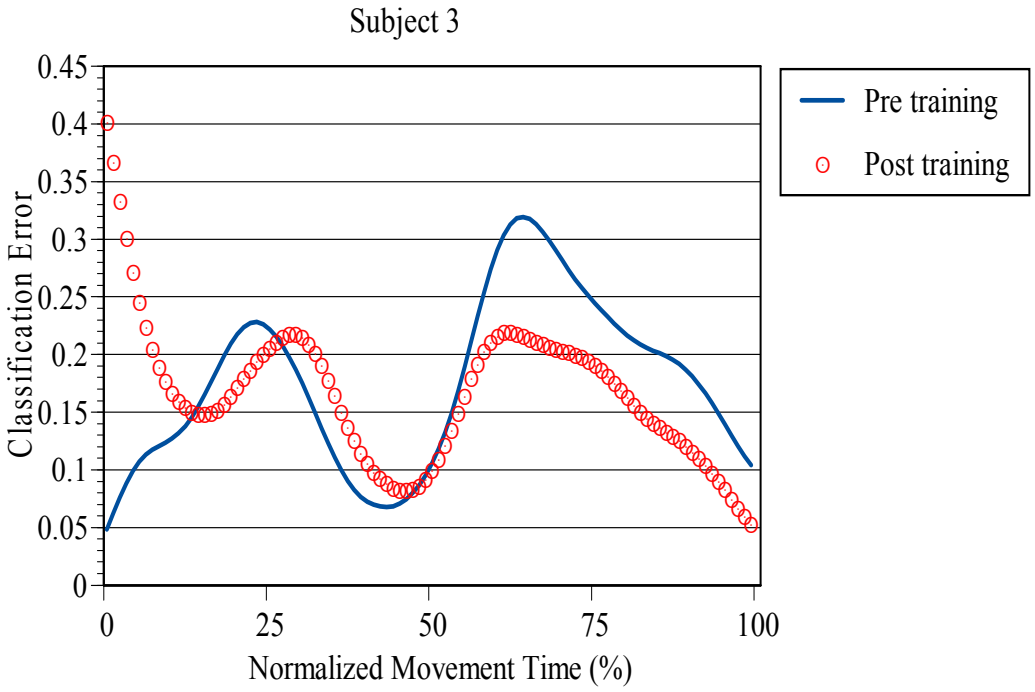


**A1** Classification error with normalized movement time of impaired hand for Subject 3.

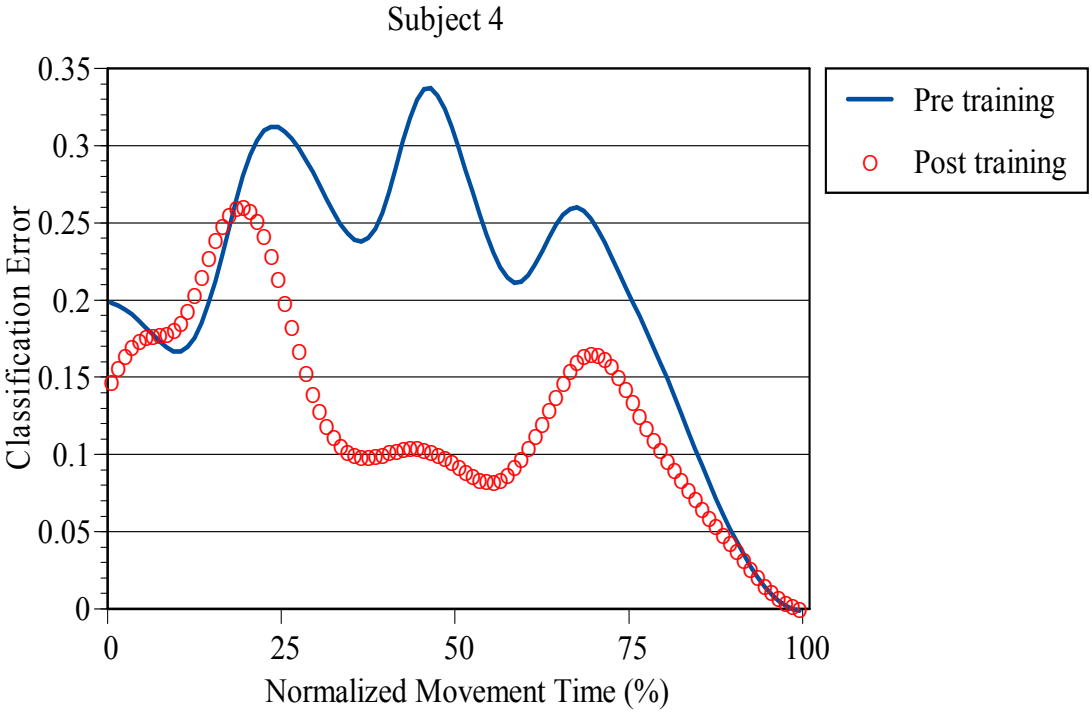


**A2** Classification error with normalized movement time of impaired hand for Subject 4.

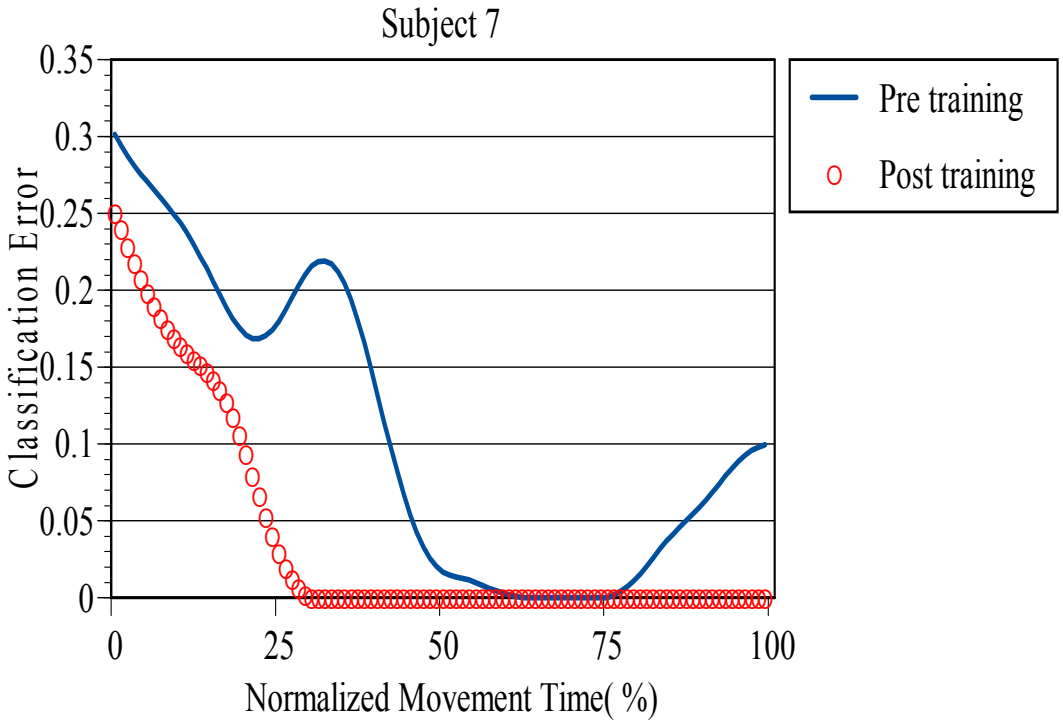


**A3** Classification error with normalized movement time of impaired hand for Subject 7.

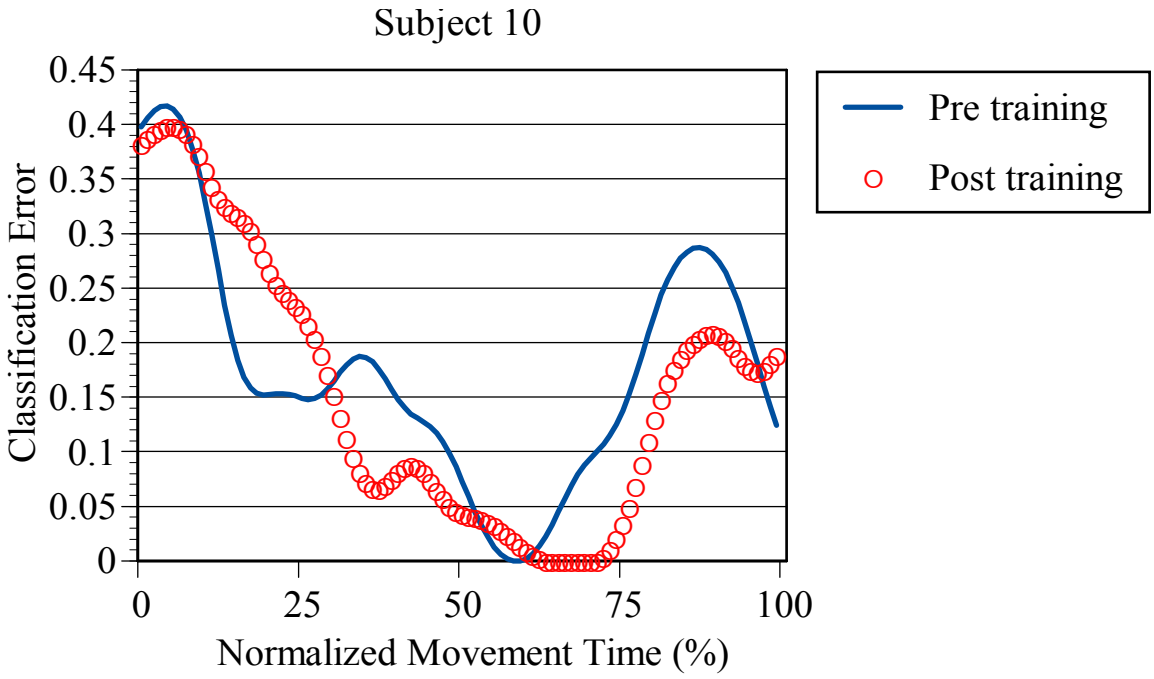


**A4** Classification error with normalized movement time of impaired hand for Subject 10.

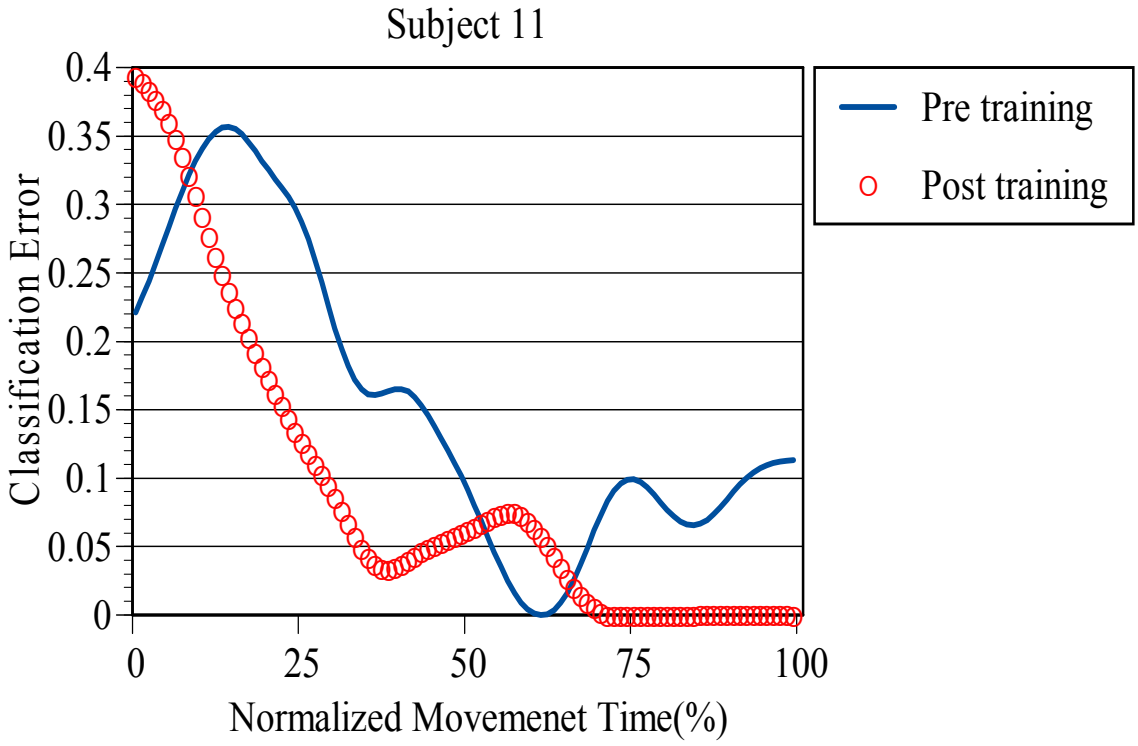


**A5** Classification error with normalized movement time of impaired hand for Subject 11.

## APPENDIX B

## SOURCE CODE FOR FORCE SENSOR

```
% Source Code for Force Data

begin=0;

fileCount = 1;

while(begin==0)

s = serial('COM1');
set(s,'BaudRate',57600,'Terminator','CR');
s.InputBufferSize = 50000;
set(s,'Stopbits',1);
set(s,'Databits',8);

fopen(s);

fprintf(s,['CB 57600']);
fprintf(s,['RS']);
fprintf(s,['CS'])
pause(1)
out = get(s,'baudrate');

sc= fscanf(s);
fprintf(s,['CD A']);
sc= fscanf(s);
readasync(s);
by=s.BytesAvailable;
if(by > 0)
temp = fread(s,by);
val = char(temp)';
end


disp('Using input command press any key but a...');
[t, keyCode,deltaSecs ]=KbWait;
disp('press a to start data collection... ');
while KbName(keyCode)~='a'
[t, keyCode,deltaSecs ]=KbWait;
end
```

```
t1=tic;
fprintf(s,['QS']);
sc= fscanf(s);
readasync(s);
disp('press b to stop data collection... ');
[t, keyCode,deltaSecs ]=KbWait;
while KbName(keyCode)~='b'
[t, keyCode,deltaSecs ]=KbWait;
end

finaltime=toc(t1)

by=s.BytesAvailable;
if(by > 0)
temp = fread(s,by);
val = char(temp)';
end

%fprintf(s,['SB']);
finaltime1=toc(t1)

t1=tic;
y=length(val);
k=1;
temp=double(val);

%for n=k:y
d=strfind(val, ',');
%end

y2=length(d);
kf=zeros(1,y2);
for n=2:y2

if val(d(n)-1)>=0&&val(d(n)-2)>=0&&val(d(n)-3)>=0&&val(d(n)-4)>=0&&val(d(n)-
5)>=0&&val(d(n)-6)>=0&&val(d(n)-7)>=0
value=val(d(n)-7:d(n)-1);
c=cellstr(value);
X = str2double(c);
kf(n)=kf(n)+X;

end

end
Testing=isnan(kf);
kf(Testing)=0;
```

```
for n=2:y2
if kf(n)==0
value2=val(d(n)-7:d(n)-2);

c=cellstr(value2);
X = str2double(c);
kf(n)=kf(n)+X;
end
end
r=(y2)/6;

datafinal=zeros((y2)/6,6);
k=2;
n=1;
m=1;

for m=m:1:r;
if m<r+1;
for k=k:k+5
if k<length(kf)+1
if n<7
datafinal(m,n)=datafinal(m,n)+kf(k);
end

n=n+1;
end
end

n=1;
k=k+1;
end
end
%%add time to matrix

sec=zeros(m,1);
k=1;
for time=finaltime/m:finaltime/m:finaltime

sec(k)=sec(k)+time;
k=k+1;
end

datafinal2=horzcat(sec,datafinal);

filename=['code_data\datafinal' num2str(fileCount) '.txt'];
```

```
save(filename,'datafinal2','-ASCII');
fileCount = fileCount+1;

fprintf(s,['^Q']);
fprintf(s,['^S']);
fclose(s);
finaltime7=toc(t1)
end
```

## APPENDIX C

## SOURCE CODE FOR CALCULATING OFFSET 1 AND ONSET 2

```
% Source Code for calculating offset1 and onset2
% Upload force sensor data
% filter data

pathname = uigetdir;
cd(pathname);
clc
subject_list = ls(pathname);

for ja =1:1

for ia=2:3
for ma=1:2
for ka=8
switch ma
case 1
impairedHand = ['left'];
case 2
impairedHand = ['right'];
end



switch ia
case 2
dir = [pathname '\pretest\' impairedHand '\'];
case 3
dir = [pathname '\posttest\' impairedHand '\'];
end

switch ka
case 1
Object = ['bigcircle'];
case 2
Object = ['bigcube'];
case 3
Object = ['smallcircle'];
case 4
Object = ['Hugecircle'];
```

```
case 5
Object = ['smallcube'];
case 6
Object = ['Pentagon'];
case 7
Object = ['Playdoh'];
case 8
Object = ['Wedge'];

end

s= [dir Object]
cd(s)
files=ls('ForceSensor*.txt');

TF=isempty(files)
if TF==1
break
end



files=cellstr(files);

if isempty(files)==1
break;
end


ttt=length(files);
ccc=1;
table=zeros(ttt,2);


for GG=1:1:ttt
x=char(files(GG,ccc));
NAME=x;
x=load(x);
original=x;


if length(x)<100
offset1=-999999;
onset2=-999999;
table(GG,1)=table(GG,1)+offset1;
table(GG,2)=table(GG,2)+onset2;
```

```
clearvars x
break
end

[B,A]=butter(3,.1,'low');
x=filtfilt(B,A,x);


for i=1

if isnan(x(i,4))==1
offset1=-999999;
onset2=-999999;
table(GG,1)=offset1;
table(GG,2)=onset2;

break
end
end



time=zeros(length(x),3);
i=1;
n=4;
r=length(x);


[min1,min2]=min(x(1:length(x)/1.5,4));
for i=min2:length(x)-2

deltaY3=(x(i+1,4))-(x(i,4));
deltaX3=(x(i+1,1)-x(i,1));
deltaY3a=(x(i+2,4))-(x(i+1,4));
deltaX3a=(x(i+2,1)-x(i+1,1));
if (deltaY3/deltaX3)<=.5 &&(deltaY3a/deltaX3a)<=.5 && x(i,4)>-700
value=i;
onset2=x(i,1);
break
end
end

for i=1:length(x)

if exist('value')==0
```

```
onset2=-999999;

end

end

if isnan(x(1,4))==0

n=1;
mo=1;
w2=3;
for m2=1:1:min2-w2
mo;
deltaY4=(x(m2+w2,4))-(x(m2,4));
deltaX4=(x(m2+w2,1)-x(m2,1));


slope4(mo,1)=m2;
slope4(mo,2)=(deltaY4/deltaX4);
mo=mo+1;

end

if exist('slope4')==0
offset1=-999999;
onset2=-999999;
table(GG,1)=offset1;
table(GG,2)=onset2;

break
end


for m3=1:1:length(slope4)
if slope4(m3,2)<-500
ansy=m3;
break
end
end


[lowest,c2]=min(slope4(:,2));   c2=ansy;
xoffset=slope4(c2);
final_offset=zeros(w2,3);
for m2=1:1:w2;
y=xoffset:1:xoffset+w2;
```

```
final_offset(m2,1)=y(m2);
final_offset(m2,2)=x(y(m2),1);
final_offset(m2,3)=x(y(m2),4);
end

offset1=final_offset(1,2);

else
offset1=-999999;
onset2=-999999;


end

table(GG,1)=offset1;
table(GG,2)=onset2;
if table(GG,2)~=-999999
if table(GG,1)>table(GG,2)
table(GG,1)=-999999;
table(GG,2)=-999999;

end
end

if table(GG,1)==table(GG,2)
table(GG,1)=-999999;
table(GG,2)=-999999;

end

clearvars slope*
clearvars x
clearvars value
clearvars onset2
clearvars offset1
end
xlswrite('offset1_onset2.xls', files, 'Times','A1');
xlswrite('offset1_onset2.xls', table, 'Times','B1');

clearvars ForceSensor*
clearvars table
end
end
end
end
```

## APPENDIX D

## UPLOAD GLOVE DATA FILES FOR CLASSIFICATION OF HAND POSTURES

```
%Upload Glove data files for classification without force times

clear all
close all


pathname1 = uigetdir;
pathname2=uigetdir;


for ia=3 %1:3
for ma=2 %1:2

for ka=3%:5
switch ma
case 1
impairedHand = ['left'];
case 2
impairedHand = ['right'];
end



switch ia
case 2
dir = [pathname1 '\pretest\' impairedHand '\'];
case 3
dir = [pathname1 '\posttest\' impairedHand '\'];
end

switch ka

case 1
Object1 = ['bigcircle'];
Object2 = ['smallcube'];
case 2
Object1 = ['bigcircle'];
Object2 = ['smallcircle'];
case 3
Object1 = ['bigcube'];
```

```
Object2 = ['bigcircle'];
case 4
Object1 = ['smallcube'];
Object2 = ['smallcircle'];
case 5
Object1 = ['smallcube'];
Object2 = ['bigcube'];
case 6
Object1 = ['bigcube'];
Object2 = ['smallcircle'];

case 7
Object1 = ['cylinder'];
Object2 = ['bigcircle'];
case 8
Object1 = ['cylinder'];
Object2 = ['smallcube'];
case 9
Object1 = ['cylinder'];
Object2 = ['bigcube'];
case 10
Object1 = ['Hugecircle'];
Object2 = ['smallcube'];
case 11
Object1 = ['Hugecircle'];
Object2 = ['bigcircle'];
case 12
Object1 = ['Hugecircle'];
Object2 = ['bigcube'];
case 13
Object1 = ['Hugecircle'];
Object2 = ['smallcircle'];
case 14
Object1 = ['Hugecircle'];
Object2 = ['Wedge'];

end
ka
clear Shape1file*
clear Shape2file*
clear force*
clear cycled*



s1cali=[dir 'calibration'];                cd(s1cali);
```

```
if strcmp('left',impairedHand)==1
shape1cali=ls('LCG*.txt');
Calitemp=load(shape1cali(1,:));
Cali2temp=load(shape1cali(2,:));
Cali3temp=load(shape1cali(3,:));
end

if strcmp('right',impairedHand)==1
shape1cali=ls('RCG*.txt');
Calitemp=load(shape1cali(1,:));
Cali2temp=load(shape1cali(2,:));
Cali3temp=load(shape1cali(3,:));
end

s1= [dir Object1];
cd(s1);

if strcmp('left',impairedHand)==1
Shape1files=ls('LCG*.txt');
Shape1files=cellstr(Shape1files);
end

if strcmp('right',impairedHand)==1
Shape1files=ls('RCG*.txt');
Shape1files=cellstr(Shape1files);
end

s2= [dir Object2];
cd(s2);
if strcmp('left',impairedHand)==1
Shape2files=ls('LCG*.txt');
Shape2files=cellstr(Shape2files);
end

if strcmp('right',impairedHand)==1
Shape2files=ls('RCG*.txt');       Shape2files=cellstr(Shape2files);
end

switch ia
case 2
dir2 = [pathname2 '\pretest\' impairedHand '\'];
case 3
dir2 = [pathname2 '\posttest\' impairedHand '\'];
end
filename3=[dir2 Object1 '\Cycled.xls'];
filename4=[dir2 Object2 '\Cycled.xls'];
```

```
[num3,txt3,raw3] = xlsread(filename3);
[num4,txt4,raw4] = xlsread(filename4);


cycledtimes1=zeros(length(txt3),3);

kk=['_1.txt';'_2.txt';'_3.txt';'_4.txt';'_5.txt';'_6.txt';'_7.txt';'_8.txt';'_9.txt';'10.txt';'11.txt';'12.t
xt'];

for i=1:size(txt3,1)

for k=1:length(kk)
val=strfind(Shape1files(i,1),kk(k,:));
val=cell2mat(val);
if isempty(val)==0
break
end
end
Shape1filesa(k,1)=Shape1files(i,1);
cycledtimes1(k,1)=num3(i,1);
cycledtimes1(k,2)=num3(i,2);
cycledtimes1(k,3)=num3(i,3);
end

kk=['r1.txt';'r2.txt';'r3.txt';'r4.txt';'r5.txt';'r6.txt';'r7.txt';'r8.txt';'r9.txt';'10.txt';'11.txt';'12.txt']
;
%



cycledtimes2=zeros(length(txt4),3

kk=['_1.txt';'_2.txt';'_3.txt';'_4.txt';'_5.txt';'_6.txt';'_7.txt';'_8.txt';'_9.txt';'10.txt';'11.txt';'12.t
xt'];

for i=1:size(txt4,1)

for k=1:length(kk)
val=strfind(Shape2files(i,1),kk(k,:));
val=cell2mat(val);
if isempty(val)==0
break
end

end
```

```
Shape2filesa(k,1)=Shape2files(i,1);
cycledtimes2(k,1)=num4(i,1);
cycledtimes2(k,2)=num4(i,2);
cycledtimes2(k,3)=num4(i,3);
end


t=1;
for i=1:length(Shape1filesa)
if iscellstr(Shape1filesa(i,:))==1
Shape1filesa1(t,:)=Shape1filesa(i,:);
t=t+1;
end
end
Shape1filesa=Shape1filesa1;
t=1;
for i=1:length(Shape2filesa)
if iscellstr(Shape2filesa(i,:))==1
Shape2filesa1(t,:)=Shape2filesa(i,:);
t=t+1;
end
end
Shape2filesa=Shape2filesa1;
for i=1:length(cycledtimes1)
if cycledtimes1(i,1)<20
cycledtimes1(i,1)=0;
end
end

for i=1:length(cycledtimes2)
if cycledtimes2(i,1)<20
cycledtimes2(i,1)=0;
end
end



check=find(cycledtimes1(1:end,1));
t=1;
for i=1:length(check)
cycledtimes1a(t,1)=cycledtimes1(check(i),1);
cycledtimes1a(t,2)=cycledtimes1(check(i),2);
cycledtimes1a(t,3)=cycledtimes1(check(i),3);
t=t+1;
end
```

```
cycledtimes1=cycledtimes1a;
check=find(cycledtimes2(1:end,1));
t=1
for i=1:length(check)
cycledtimes2a(t,1)=cycledtimes2(check(i),1);
cycledtimes2a(t,2)=cycledtimes2(check(i),2);
cycledtimes2a(t,3)=cycledtimes2(check(i),3);
t=t+1;
end

cycledtimes2=cycledtimes2a;
v=1;

min1=min(cycledtimes1(:,1));
sub=min1-1;

cd(s1)
Data1=[];
OriginalData1=[];
i2=1;
for i=1:size(cycledtimes1,1)
clear x1
clear xtemp
clear nonzeroentry
x=load(char(Shape1filesa(i)));
[b,a]=butter(2,1/50);
x=filtfilt(b,a,x);
x=calibration(x,Calitemp,Cali2temp,Cali3temp);



if cycledtimes1(i,1)~=-999999

if i2<size(cycledtimes1,1)+1
if length(x)>=(cycledtimes1(i,2))
if cycledtimes1(i,2)>0
x1=x(cycledtimes1(i,1)-sub:floor(cycledtimes1(i,2)),:);
end
end
end

if i2<size(cycledtimes1,1)+1

if cycledtimes1(i,2)<0
x1=x(cycledtimes1(i,1)-sub:end,:);
end
```

```
end


if i2<size(cycledtimes1,1)+1

if size(x,1)<(cycledtimes1(i,2))
x1=x(cycledtimes1(i,1)-sub:end,:);
end

end


if size(x1,1)<100
x4=zeros(100,20);
x4(1:size(x1,1),:)=x1(:,:);
for ii=size(x1,1)+1:length(x4)
x4(ii,:)=x1(size(x1,1),:);
end
x1=x4;
end

x2=(size(x1,1)/100);
x3=zeros(100,20);
for norm=1:100
x3(norm,:)=(x1(floor(x2*norm),:));
end
Data1=cat(3,Data1,x3);

else
CONTINUE
end
i2=i2+1;


x=x(cycledtimes1(i,1)-sub:end,:);
if size(x,1)<500
x4test=zeros(500,20);
x4test(1:size(x,1),:)=x(:,:);


for ii=size(x,1)+1:length(x4test)
x4test(ii,:)=x(length(x),:);
end
x=x4test;
end
```

```
xx=(size(x,1)/500);
xxx=zeros(500,20);
for normx=1:500
xxx(normx,:)=(x(floor(xx*normx),:));
end
OriginalData1=cat(3,OriginalData1,xxx);
end

min2=min(cycledtimes2(:,1));
sub2=min2-1;

cd(s2)
Data2=[];
i2=1;

OriginalData2=[];
for i=1:size(cycledtimes2,1)
clear x1
clear xtemp
clear nonzeroentry
x=load(char(Shape2filesa(i)));
[b,a]=butter(2,1/50);
x=filtfilt(b,a,x);
x=calibration(x,Calitemp,Cali2temp,Cali3temp);
if cycledtimes2(i,1)~=-999999


if i2<size(cycledtimes2,1)+1
if size(x,1)>=(cycledtimes2(i,2))
if cycledtimes2(i,2)>0
x1=x(cycledtimes2(i,1)-sub2:floor(cycledtimes2(i,2)),:);
end
end
end

if i2<size(cycledtimes2,1)+1

if cycledtimes2(i,2)<0
x1=x(cycledtimes2(i,1)-sub2:end,:);
end

end

if i2<size(cycledtimes2,1)+1
```

```
if size(x,1)<(cycledtimes2(i,2))
x1=x(cycledtimes2(i,1)-sub2:end,:);
end

end
% end

if size(x1,1)<100
x4=zeros(100,20);
x4(1:size(x1,1),:)=x1(:,:);
for ii=size(x1,1)+1:length(x4)
x4(ii,:)=x1(size(x1,1),:);
end
x1=x4;
end

x2=(size(x1,1)/100);
x3=zeros(100,20);
for norm=1:100
x3(norm,:)=(x1(floor(x2*norm),:));
end
Data2=cat(3,Data2,x3);
else
CONTINUE
end
i2=i2+1;

x=x(cycledtimes2(i,1)-sub2:end,:);
x=x(1:end,:);
if size(x,1)<500
x4test=zeros(500,20);
x4test(1:size(x,1),:)=x(:,:);


for ii=size(x,1)+1:length(x4test)
x4test(ii,:)=x(size(x,1),:);
end
x=x4test;

end
xx=(size(x,1)/500);
xxx=zeros(500,20);
for normx=1:500
xxx(normx,:)=(x(floor(xx*normx),:));
end
OriginalData2=cat(3,OriginalData2,xxx);
```

```
end

FinalData=cat(3,Data1,Data2);
OriginalData=cat(3,OriginalData1,OriginalData2);
NofTri=[size(Data1,3);size(Data2,3)];

FinalData1=FinalData(:,:,:);

FinalData1a=FinalData(:,5,:);
FinalData1a1=FinalData(:,6,:);
FinalData1b=FinalData(:,8:10,:);
FinalData1c=FinalData(:,12:14,:);
FinalData1d=FinalData(:,16:18,:);
FinalData11=cat(2,FinalData1a,FinalData1a1,FinalData1b,FinalData1c,FinalData1d);

Errors=LinDiscrimTMS(FinalData11,NofTri);
Mean_Errors=mean(Errors);
[b,a]=butter(2,.1);
Errorsfilt=filtfilt(b,a,Errors);

MCP1=[];
for i=1:size(FinalData,3)
MCP1=cat(2,MCP1,FinalData(:,6,i));
end


MCP1whole=[];
for i=1:size(OriginalData,3)
MCP1whole=cat(2,MCP1whole,OriginalData(:,6,i));
end

ABD1=[];
for i=1:size(FinalData,3)
ABD1=cat(2,ABD1,FinalData(:,8,i));
end


ABD1whole=[];
for i=1:size(OriginalData,3)
ABD1whole=cat(2,ABD1whole,OriginalData(:,8,i));
end


if ia==2 && ma==1
pretestErrors_left=(Errorsfilt);
```

```
end

if ia==3 && ma==1
posttestErrors_left=(Errorsfilt);
end

if ia==2 && ma==2
pretestErrors_right=(Errorsfilt);
end

if ia==3 && ma==2
posttestErrors_right=(Errorsfilt);
end

end
end

clear test1
figure(3)
yy=size(OriginalData,3);
test1(:,1:yy,1)=OriginalData(:,10,:);
plot(test1)

clear test1
figure(4)
yy=size(FinalData11,3);
test1(:,1:yy,1)=FinalData11(:,5,:);   % iABD
plot(test1)

end

figure(1);hold on
plot(pretestErrors_left,'linewidth',2)
hold on
plot(posttestErrors_left,'r','linewidth',2)
hold on
plot(pretestErrors_right,'g','linewidth',2)
hold on
plot(posttestErrors_right,'m','linewidth',2)
legend('pretest_Left','posttest_left','pretest_Right','posttest_Right';
```

## APPENDIX E

## UPLOAD GLOVE AND FORCE DATA FOR CLASSIFICATION OF HAND POSTURES FOR VR SUBJECTS

```
% Upload glove data and force data for classification of VR subjects

s1= [dir Object1 '\offset1_onset2.xls']

s1cali=[dir 'calibration'                cd(s1cali);
if strcmp('left',impairedHand)==1
shape1cali=ls('LCG*.txt');
Calitemp=load(shape1cali(1,:));
Cali2temp=load(shape1cali(2,:));
Cali3temp=load(shape1cali(3,:));
end

if strcmp('right',impairedHand)==1
shape1cali=ls('RCG*.txt');
Calitemp=load(shape1cali(1,:));
Cali2temp=load(shape1cali(2,:));
Cali3temp=load(shape1cali(3,:));
end

s2= [dir Object2 '\offset1_onset2.xls']
filename1=s1;
filename2=s2;


sheet='Times';
[num1,txt1,raw1] = xlsread(filename1,sheet);
[num2,txt2,raw2] = xlsread(filename2,sheet);
s1= [dir Object1];
cd(s1);

if strcmp('left',impairedHand)==1
Shape1files=ls('LCG*.txt');
Shape1files=cellstr(Shape1files);
end

if strcmp('right',impairedHand)==1
Shape1files=ls('RCG*.txt');
Shape1files=cellstr(Shape1files);
end
```

```
s2= [dir Object2];
cd(s2);
if strcmp('left',impairedHand)==1
Shape2files=ls('LCG*.txt');
Shape2files=cellstr(Shape2files);
end

if strcmp('right',impairedHand)==1
Shape2files=ls('RCG*.txt');
Shape2files=cellstr(Shape2files);
end

switch ia
case 2
dir2 = [pathname2 '\pretest\' impairedHand '\'];
case 3
dir2 = [pathname2 '\posttest\' impairedHand '\'];
end
filename3=[dir2 Object1 '\Cycled.xls'];
filename4=[dir2 Object2 '\Cycled.xls'];

%read cycled file
[num3,txt3,raw3] = xlsread(filename3);
[num4,txt4,raw4] = xlsread(filename4);


cycledtimes1=zeros(length(txt3),3);

kk=['_1.txt';'_2.txt';'_3.txt';'_4.txt';'_5.txt';'_6.txt';'_7.txt';'_8.txt';'_9.txt';'10.txt';'11.txt';'12.t
xt'];

for i=1:length(txt3)

for k=1:length(kk)
val=strfind(Shape1files(i,1),kk(k,:));
val=cell2mat(val);
if isempty(val)==0
break
end
end
Shape1filesa(k,1)=Shape1files(i,1);
cycledtimes1(k,1)=num3(i,1);
cycledtimes1(k,2)=num3(i,2);
cycledtimes1(k,3)=num3(i,3);
end
```

```
forcetimes1=zeros(length(txt1),2);
kk=['r1.txt';'r2.txt';'r3.txt';'r4.txt';'r5.txt';'r6.txt';'r7.txt';'r8.txt';'r9.txt';'10.txt';'11.txt';'12.txt']
;

for i=1:size(txt1,1)

for k=1:length(kk)
val=strfind(raw1(i,1),kk(k,:));
val=cell2mat(val);
if isempty(val)==0
break
end
end

forcetimes1(k,1)=num1(i,1);
forcetimes1(k,2)=num1(i,2);

end


cycledtimes2=zeros(length(txt4),3);

kk=['_1.txt';'_2.txt';'_3.txt';'_4.txt';'_5.txt';'_6.txt';'_7.txt';'_8.txt';'_9.txt';'10.txt';'11.txt';'12.t
xt'];

for i=1:size(txt4,1)

for k=1:length(kk)
val=strfind(Shape2files(i,1),kk(k,:));
val=cell2mat(val);
if isempty(val)==0
break
end

end
Shape2filesa(k,1)=Shape2files(i,1);
cycledtimes2(k,1)=num4(i,1);
cycledtimes2(k,2)=num4(i,2);
cycledtimes2(k,3)=num4(i,3);
end


forcetimes2=zeros(length(txt2),2);
kk=['r1.txt';'r2.txt';'r3.txt';'r4.txt';'r5.txt';'r6.txt';'r7.txt';'r8.txt';'r9.txt';'10.txt';'11.txt';'12.txt']
;
```

```
for i=1:length(txt2)

for k=1:length(kk)
val=strfind(raw2(i,1),kk(k,:));
val=cell2mat(val);
if isempty(val)==0
break
end
end

forcetimes2(k,1)=num2(i,1);
forcetimes2(k,2)=num2(i,2);

end


t=1;
for i=1:length(Shape1filesa)
if iscellstr(Shape1filesa(i,:))==1
Shape1filesa1(t,:)=Shape1filesa(i,:);
t=t+1;
end
end
Shape1filesa=Shape1filesa1;
t=1;
for i=1:length(Shape2filesa)
if iscellstr(Shape2filesa(i,:))==1
Shape2filesa1(t,:)=Shape2filesa(i,:);
t=t+1;
end
end
Shape2filesa=Shape2filesa1;

check=find(forcetimes1(1:end,1));
t=1
for i=1:length(check)
forcetimes1a(t,1)=forcetimes1(check(i),1);
forcetimes1a(t,2)=forcetimes1(check(i),2);
t=t+1;
end

forcetimes1=forcetimes1a;
check=find(forcetimes2(1:end,1));
t=1;
for i=1:length(check)
```

```
forcetimes2a(t,1)=forcetimes2(check(i),1);
forcetimes2a(t,2)=forcetimes2(check(i),2);
t=t+1;
end

forcetimes2=forcetimes2a;

check=find(cycledtimes1(1:end,1));
t=1;
for i=1:length(check)
cycledtimes1a(t,1)=cycledtimes1(check(i),1);
cycledtimes1a(t,2)=cycledtimes1(check(i),2);
cycledtimes1a(t,3)=cycledtimes1(check(i),3);
t=t+1;
end

cycledtimes1=cycledtimes1a;
check=find(cycledtimes2(1:end,1));
t=1;
for i=1:length(check)
cycledtimes2a(t,1)=cycledtimes2(check(i),1);
cycledtimes2a(t,2)=cycledtimes2(check(i),2);
cycledtimes2a(t,3)=cycledtimes2(check(i),3);
t=t+1;
end

cycledtimes2=cycledtimes2a;
v=1;
for i=1:size(cycledtimes1,1)
if cycledtimes1(i,1)>0
newvector1(v,1)=cycledtimes1(i,1);
v=v+1;
end
end
av1=mean(newvector1);

v=1;
for i=1:size(cycledtimes2,1)
if cycledtimes2(i,1)>0
newvector2(v,1)=cycledtimes2(i,1);
v=v+1;
end
end
av2=mean(newvector2);
cd(s1)
Data1=[];
```

```
OriginalData1=[];
i2=1;
for i=1:size(cycledtimes1,1)
clear x1
clear xtemp
clear nonzeroentry
x=load(char(Shape1filesa(i)));
[b,a]=butter(2,1/50);
x=filtfilt(b,a,x);
x=calibration(x,Calitemp,Cali2temp,Cali3temp);

if cycledtimes1(i,1)~=-999999

sub=min(cycledtimes1(:,1));
sub=sub-1;
if i2<size(forcetimes1,1)+1
if forcetimes1(i2,1)>0 && size(x,1)>=floor((forcetimes1(i,1)*100))
x1=x(cycledtimes1(i,1)-sub:floor(forcetimes1(i,1)*100),:);
end
end


if i2<size(forcetimes1,1)+1
if length(x)>=cycledtimes1(i,1)&&cycledtimes1(i,2)>0
if forcetimes1(i2,1)>0 && size(x,1)<floor(forcetimes1(i,1)*100)
x1=x(cycledtimes1(i,1)-sub:cycledtimes1a(i,2),:);
end
end
end
if i2<size(forcetimes1,1)+1
if forcetimes1(i2,2)<0 && size(x,1)>=(cycledtimes1(i,2))
x1=x(cycledtimes1(i,1)-sub:cycledtimes1a(i,2),:);
end
end

if i2<size(cycledtimes1,1)+1 && i2>=size(forcetimes1,1)+1
if length(x)>=(cycledtimes1(i,2))
if cycledtimes1(i,2)>0
x1=x(cycledtimes1(i,1)-sub:floor(cycledtimes1a(i,2)),:);
end
end
end

if i2<size(cycledtimes1,1)+1 && i2>=size(forcetimes1,1)+1

if cycledtimes1(i,2)<0
```

```
x1=x(cycledtimes1(i,1)-sub:end,:);
end

end


if size(x1,1)<100
x4=zeros(100,20);
x4(1:size(x1,1),:)=x1(:,:);
for ii=size(x1,1)+1:length(x4)
x4(ii,:)=x1(size(x1,1),:);
end
x1=x4;
end

x2=(size(x1,1)/100);
x3=zeros(100,20);
for norm=1:100
x3(norm,:)=(x1(floor(x2*norm),:));
end
Data1=cat(3,Data1,x3);

else
CONTINUE
end
i2=i2+1;


x=x(cycledtimes1(i,1)-sub:end,:);
if size(x,1)<500
x4test=zeros(500,20);
x4test(1:size(x,1),:)=x(:,:);


for ii=size(x,1)+1:length(x4test)
x4test(ii,:)=x(length(x),:);
end
x=x4test;
end

xx=(size(x,1)/500);
xxx=zeros(500,20);
for normx=1:500
xxx(normx,:)=(x(floor(xx*normx),:));
end
OriginalData1=cat(3,OriginalData1,xxx);
```

```
end



cd(s2)
Data2=[];
i2=1;

OriginalData2=[];
for i=1:size(cycledtimes2,1)
clear x1
clear xtemp
clear nonzeroentry
x=load(char(Shape2filesa(i)));
[b,a]=butter(2,1/50);
x=filtfilt(b,a,x);
x=calibration(x,Calitemp,Cali2temp,Cali3temp);
if cycledtimes2(i,1)~=-999999

sub2=min(cycledtimes2(:,1));
sub2=sub2-1;

if i2<size(forcetimes2,1)+1
if forcetimes2(i2,1)>0 && length(x)>=floor((forcetimes2(i,1)*100))
x1=x(cycledtimes2(i,1)-sub2:floor(forcetimes2(i,1)*100),:);
end
end


if i2<size(forcetimes2,1)+1
if length(x)>=cycledtimes2(i,1)&&cycledtimes2(i,2)>0
if forcetimes2(i2,1)>0 && length(x)<floor(forcetimes2(i,1)*100)
x1=x(cycledtimes2(i,1)-sub2:cycledtimes2a(i,2),:);
end
end
end
if i2<size(forcetimes2,1)+1
if forcetimes2(i2,2)<0 && length(x)>=(cycledtimes2(i,2))
x1=x(cycledtimes2(i,1)-sub2:cycledtimes2a(i,2),:);
end
end


if i2<size(cycledtimes2,1)+1 && i2>=size(forcetimes2,1)+1
if length(x)>=(cycledtimes2(i,2))
if cycledtimes2(i,2)>0
```

```
x1=x(cycledtimes2(i,1)-sub2:floor(cycledtimes2a(i,2)),:);
end
end
end

if i2<size(cycledtimes2,1)+1 && i2>=size(forcetimes2,1)+1

if cycledtimes2(i,2)<0
x1=x(cycledtimes2(i,1)-sub2:end,:);
end

end

%if isempty('x1')==1
if size(x1,1)<100
x4=zeros(100,20);
x4(1:size(x1,1),:)=x1(:,:);
for ii=size(x1,1)+1:length(x4)
x4(ii,:)=x1(size(x1,1),:);
end
x1=x4;
end

x2=(size(x1,1)/100);
x3=zeros(100,20);
for norm=1:100
x3(norm,:)=(x1(floor(x2*norm),:));
end
Data2=cat(3,Data2,x3);
else
CONTINUE
end
i2=i2+1;

x=x(cycledtimes2(i,1)-sub2:end,:);
x=x(1:end,:);
if size(x,1)<500
x4test=zeros(500,20);
x4test(1:size(x,1),:)=x(:,:);


for ii=size(x,1)+1:length(x4test)
x4test(ii,:)=x(size(x,1),:);
end
x=x4test;
```

```
end
xx=(size(x,1)/500);
xxx=zeros(500,20);
for normx=1:500
xxx(normx,:)=(x(floor(xx*normx),:));
end
OriginalData2=cat(3,OriginalData2,xxx);
end
```

## APPENDIX F

## SOURCE CODE TO RETRIEVE GRASPING TIMES AND TOTAL MOVEMENT TIMES FILES

```
% Source Code to retrieve grasping times and total movement times files

clear all
close all
pathname1 = uigetdir;

for ia=2:3
for ma=1

for ka=1:5
switch ma
case 1
impairedHand = ['left'];
case 2
impairedHand = ['right'];
end


switch ia
case 2
dir = [pathname1 '\pretest\' impairedHand '\'];
case 3
dir = [pathname1 '\posttest\' impairedHand '\'];
end

switch ka

case 1
Object1 = ['Hugecircle'];
case 2
Object1 = ['bigcircle'];

case 3
Object1 = ['smallcircle'];

case 4
Object1 = ['bigcube'];

case 5
```

```
Object1 =  ['smallcube'];

case 6
Object1 = ['cylinder'];

end


filename1=[dir Object1 '\Cycled.xls'];
[num3,txt3,raw3] = xlsread(filename1);

h=size(num3,1)

if ia==2
for i=1:h
pretest(i,ka*4-1)=num3(i,3)
pretest(i,ka*4-2)=num3(i,2)
pretest(i,ka*4-3)=num3(i,1)
end
end

if ia==3
for i=1:h
posttest(i,ka*4-1)=num3(i,3)
posttest(i,ka*4-2)=num3(i,2)
posttest(i,ka*4-3)=num3(i,1)
end
end

end
end
end
```

## REFERENCES


[1] J. R. Napier, "The prehensile movements of the human hand," *J Bone Joint Surg Br,* vol. 38-B, pp. 902-13, Nov 1956.

[2] ASSH. (2011, Accessed January 15, 2012). *Hand Anatomy*. Available: http://www.assh.org/Public/HandAnatomy/Pages/default.aspx

[3] U. Castiello, "The neuroscience of grasping," *Nat Rev Neurosci,* vol. 6, pp. 726-36, Sep 2005.

[4] M. Jeannerod, "Visuomotor channels: Their integration in goal-directed prehension," *Human Movement Science,* vol. 18, pp. 201-218, 1999.

[5] E. R. Kandel, J. H. Schwartz, and T. M. Jessell, *Principles of neural science*, 4th ed. New York: McGraw-Hill, Health Professions Division, 2000.

[6] A. M. Wing, A. Turton, and C. Fraser, "Grasp size and accuracy of approach in reaching," *J Mot Behav,* vol. 18, pp. 245-60, Sep 1986.

[7] P. M. Fitts, "The information capacity of the human motor system in controlling the amplitude of movement," *J Exp Psychol,* vol. 47, pp. 381-91, Jun 1954.

[8] R. J. Bootsma, R. G. Marteniuk, C. L. MacKenzie, and F. T. Zaal, "The speed-accuracy trade-off in manual prehension: effects of movement amplitude, object size and object width on kinematic characteristics," *Exp Brain Res,* vol. 98, pp. 535-41, 1994.

[9] A. H. Mason and H. Carnahan, "Target viewing time and velocity effects on prehension," *Exp Brain Res,* vol. 127, pp. 83-94, Jul 1999.

[10] A. C. Roy, Y. Paulignan, M. Meunier, and D. Boussaoud, "Prehension movements in the macaque monkey: effects of object size and location," *J Neurophysiol,* vol. 88, pp. 1491-9, Sep 2002.

[11] M. Santello and J. F. Soechting, "Gradual molding of the hand to object contours," *J Neurophysiol,* vol. 79, pp. 1307-20, Mar 1998.

[12] L. F. Schettino, S. V. Adamovich, and H. Poizner, "Effects of object shape and visual feedback on hand configuration during grasping," *Exp Brain Res,* vol. 151, pp. 158-66, Jul 2003.

[13] L. F. Schettino, V. Rajaraman, D. Jack, S. V. Adamovich, J. Sage, and H. Poizner, "Deficits in the evolution of hand preshaping in Parkinson's disease," *Neuropsychologia,* vol. 42, pp. 82-94, 2004.

[14] M. Ralph L. Sacco, MD, FAAN, FAHA, Chair; Thomas R. Frieden, MD, MPH, Co-Chair; Drew E. Blakeman, MS; Edward C. Jauch, MD, MS, FAHA; Stephanie Mohl, "What the Million Hearts Initiative Means for Stroke: A Presidential Advisory From the American Heart Association/American Stroke Association," *Stroke,* vol. 43, pp. 924-928, 2012.

[15] M. Alt Murphy, C. Willen, and K. S. Sunnerhagen, "Kinematic variables quantifying upper-extremity performance after stroke during reaching and drinking from a glass," *Neurorehabil Neural Repair,* vol. 25, pp. 71-80, Jan 2011.

[16] P. Paulette M. van Vliet, Martin R. Sheridan, PhD, "Coordination Between Reaching and Grasping in Patients With Hemiparesis and Healthy Subjects," *Arch Phys Med Rehabil,* vol. 88, pp. 1325-31, 2007.

[17] N. Dancause and R. J. Nudo, "Shaping plasticity to enhance recovery after injury," *Prog Brain Res,* vol. 192, pp. 273-95, 2011.

[18] A. J. Bastian, "Understanding sensorimotor adaptation and learning for rehabilitation," *Curr Opin Neurol,* vol. 21, pp. 628-33, Dec 2008.

[19] A. S.-C. a. M. H. Woollacott, *Motor Control: Translating Research into Clinical Practice, Third Edition*. Philadelphia, Pennsylvania: Lippincott Williams & Wilkins, 2007.

[20] G. F. Wittenberg, R. Chen, K. Ishii, K. O. Bushara, S. Eckloff, E. Croarkin, E. Taub, L. H. Gerber, M. Hallett, and L. G. Cohen, "Constraint-induced therapy in stroke: magnetic-stimulation motor maps and cerebral activation," *Neurorehabil Neural Repair,* vol. 17, pp. 48-57, Mar 2003.

[21] A. Sunderland, D. J. Tinson, E. L. Bradley, D. Fletcher, R. Langton Hewer, and D. T. Wade, "Enhanced physical therapy improves recovery of arm function after

stroke. A randomised controlled trial," *J Neurol Neurosurg Psychiatry,* vol. 55, pp. 530-5, Jul 1992.

[22] H. I. Krebs, N. Hogan, M. L. Aisen, and B. T. Volpe, "Robot-aided neurorehabilitation," *IEEE Trans Rehabil Eng,* vol. 6, pp. 75-87, Mar 1998.

[23] A. S. Merians, H. Poizner, R. Boian, G. Burdea, and S. Adamovich, "Sensorimotor training in a virtual reality environment: does it improve functional recovery poststroke?," *Neurorehabil Neural Repair,* vol. 20, pp. 252-67, Jun 2006.

[24] A. S. Merians, G. G. Fluet, Q. Qiu, S. Saleh, I. Lafond, A. Davidow, and S. V. Adamovich, "Robotically facilitated virtual rehabilitation of arm transport integrated with finger movement in persons with hemiparesis," *J Neuroeng Rehabil,* vol. 8, p. 27, 2011.

[25] G. G. F. A S Merians, Q Qiu, S Saleh, I Lafond, S V Adamovich, "Integrated arm and hand training using adaptive robotics and virtual reality simulation," *Proc. 8th Intl Conf. Disability, Virtual Reality and Associated Technologies,* vol. 31, pp. 131-137, 2010.

[26] R. Boian, A. Sharma, C. Han, A. Merians, G. Burdea, S. Adamovich, M. Recce, M. Tremaine, and H. Poizner, "Virtual reality-based post-stroke hand rehabilitation," *Stud Health Technol Inform,* vol. 85, pp. 64-70, 2002.

[27] P. A. C. Steven L. Wolf, Michael Ellis, Audrey Link Archer, Bryn Morgan, and imee Piacentino, "Assessing Wolf motor function test as outcome measure for research in patients after stroke," *Stroke,* vol. 32, pp. 1635-1639, 2001.

[28] N. T. R.H. Jebsen, R.B. Trieschmann, M.J. Trotter, and L.A. Howard, "An objective and standardized test of hand function," *Arch Phys Med Rehabil,* vol. 50, pp. 311-319, 1969.

[29] C. G. S. LLC, "Virtual Hand User's Guide," vol. 2.7, ed, 2009.

[30] A. I. Automation, "F/T Controller (CTL/CTLJ/CON) :Six- Axis Force/Torque Sensor System," p. 223, 2010.

[31] S. Ralph B. D' Agostino, Lisa M. Sullivan, Alexa S. Beiser, *Introductory Applied Biostatistics*. Florence, Kentucky: Thomson Brooks/Cole, 2006.

[32] A. R. Webb, "Linear Discriminant Analysis," in *Statistical Pattern Recognition*, ed Hoboken, New Jersey: John Wiley & Sons, Ltd, 2003, pp. 123-168.

[33] G. A. M. a. S. L. Hershberger, *Multivariate Statistical Methods: A First Course*. Mahwah, New Jersey: Lawrence Erlbaum Associates, Inc., 1997.

[34] SPSS, "Discriminant Analysis," ed, pp. 589-604.

[35] J. N. Ingram, K. P. Kording, I. S. Howard, and D. M. Wolpert, "The statistics of natural hand movements," *Exp Brain Res,* vol. 188, pp. 223-36, Jun 2008.